Table 1. **Clinical Characteristics of the Subjects at Baseline**

Variables	Male (n=2440)	Female (n=734)
Age, years	45.5±10.6	43.0±9.7
Body weight, kg	69.4±9.8	54.6±8.5
Body mass index, kg/m^2	24.3±3.1	22.3±3.5
Waist circumference, cm	84.9±8.3	78.2±10.0
Triglyceride, mg/dL	174.1±123.1	105.3±75.1
HDL cholesterol, mg/dL	53.7±14.7	65.4±15.4
LDL cholesterol, mg/dL	115.4±29.7	111.7±28.7
Systolic blood pressure, mm Hg	130.3±15.7	119.2±15.6
Diastolic blood pressure, mm Hg	80.1±11.8	71.9±11.9
Plasma glucose, mg/dL	105.3±33.4	98.3±24.7

Data are means±SD. HDL, high-density lipoprotein; LDL, low-density lipoprotein.

In Amagasaki City Office, 7 fatal atherosclerotic vascular events were recorded from year 1995 to 2002 in all -4,000 employees. In addition to the health costs, the insurance costs had also been increasing. Therefore, prevention of CVD was an important and urgent task for the city and employer. To this end, measurement of waist circumference in annual health checkup commenced in year 2003 in these employees, based on the concept that visceral fat accumulation causes the metabolic syndrome. According to the results of the health checkup, a health education "Hokenshido" program, using "Where am I?" chart on the way to develop atherosclerosis, was applied by the medical staff to prevent further development of lifestyle-related diseases and CVD for each subject. We reported previously that the decrease in visceral fat within one year correlated with the decrease in the number of metabolic risk factors (raised blood pressure, dyslipidemia and glucose intolerance) and increase in serum levels of adiponectin (8-17).

The aim of this study was to evaluate the effect of this whole program on the incidence of metabolic syndrome for each year and for each generation of males and females.

Materials and Methods

Participants

This urban area study group comprised 3,174 Japanese [2,440 males (45.9±10.6 years, mean ± SD), 734 females (43.0±9.7 years)] who were employees of the Amagasaki City Office, Hyogo, Japan and had completed the Government-funded annual health checkup every year from 2003 to 2005. The clinical characteristics of the study participants at baseline in year 2003 are shown in Table 1. Of the entire group, 118 (3.7%), 337 (10.6%), and 115 (3.6%) individuals were under treatment for dyslipidemia, hypertension, or diabetes, respectively, at baseline.

All participants gave full informed consent to participate in the study and ethical approval was obtained from committee on the Ethics of Human Research of Osaka University. This trial is registered with number UMIN 000002391 (the Amagasaki Visceral Fat Study).

Anthropometry and laboratory measurements

Height and weight were measured in the standing position. Body mass index was calculated as weight (kg) divided by the square of height in meters (m^2). Waist circumference at the umbilical level was measured in cm with a non-stretchable tape in the late exhalation phase at standing position (18). Systolic and diastolic blood pressure values were measured in the sitting position. Blood was withdrawn fasting or postprandial condition. Biochemical variables were measured with a conventional automated analyzer.

Assessment of risk factors

We defined the metabolic syndrome according to the guidelines for the diagnosis in Japan (19). Abdominal obesity, waist circumference equal to or greater than 85 cm in men or greater than 90 cm in women plus the presence of at least two of the following abnormalities: 1) dyslipidemia; a serum fast triglyceride level over 150 mg/dL and/or a serum high-density lipoprotein (HDL) cholesterol level less than 40 mg/dL, 2) hypertension; systolic blood pressure over 130 mmHg and/or diastolic blood pressure over 85 mmHg and 3) high glucose; serum fast glucose level over 110 mg/dL. Subjects who received specific treatment(s) for each of the above metabolic risk factors were considered positive for that factor. It means that, those who had a risk factor without treatment and those who were on treatment were also included as study subjects. In the case that blood samples were not obtained after >8-hour fasting, we modified 1) to 1)' dyslipidemia; postprandial triglyceride level over 200 mg/dL (20, 21) and/or a serum high-density lipoprotein (HDL) cholesterol level less than 40 mg/dL, 3) to 3)' as high glucose; postprandial serum glucose level over 140 mg/dL (22).

Detailed examination

Oral glucose tolerance test, bicycle ergometer stress test, and carotid artery echography were performed in those subjects with risk factor(s) based on the recommendation of the team physician.

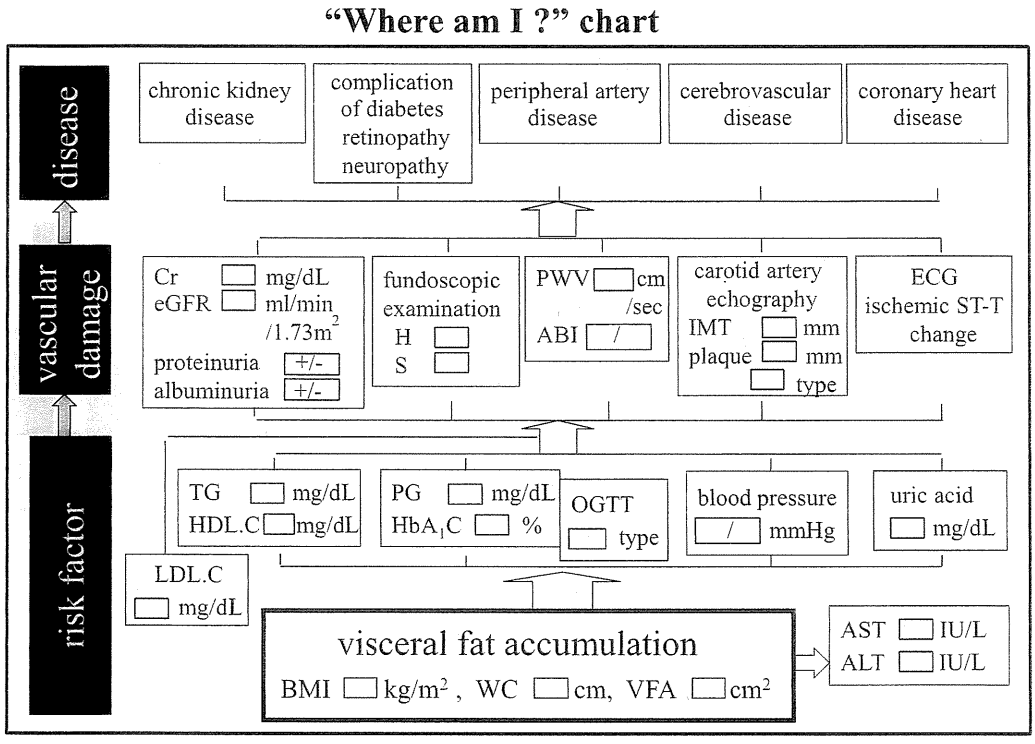

Figure 1. **The "Where am I?" chart. All results were transferred into this chart for the individual subject. The metabolic risk factors of vascular damage were displayed at the bottom part of the chart. The results of detailed examination to estimate the current condition of vascular damage were set at the middle of the chart. The status of presence or absence of diseases such as cardiovascular diseases (CVD) was displayed at the top of the chart. BMI: body mass index, WC: waist circumference, VFA: visceral fat area, LDL.C: low-density lipoprotein cholesterol, TG: triglyceride, HDL.C: high-density lipoprotein cholesterol, PG: plasma glucose, OGTT: oral glucose tolerance test, Cr: serum creatinine, eGFR: estimated glomerular filtration rate, PWV: pulse wave velocity, ABI: ankle-brachial index, IMT: intima media thickness**

Health guidance ("Hokenshido")

After the health checkup, all of the participants receive the results of the health checkup and "Where am I?" chart (Fig. 1). To enhance understanding, all of the subjects were informed and given the opportunity to attend lectures by public health nurses and medical doctors.

In "Where am I?" chart, the metabolic risk factors of vascular damage were displayed at the bottom part of the chart. The results of detailed examination to estimate the current condition of vascular damage were put at the middle (of the chart). The status of presence or absence of diseases such as CVD was displayed at the top (of the chart). The placement of visceral fat accumulation at the bottom (part) implicates that metabolic risk factors, such as dyslipidemia, hyperglycemia, hypertension, and hyperuricemia are "the tip of the iceberg", and that visceral fat accumulation (dysregulation of adipocytokines in abdominal and visceral obesity) should induce the development of the risk factors, leading to atherosclerotic CVD and chronic kidney disease. Through this chart stream, the subjects having visceral fat accumulation can imagine their assumable stage for vascular damage, and be encouraged to alter their problematic lifestyle toward reducing visceral fat and cardiovascular risks. Such subjects are spontaneously helped to identify themselves as high risk subjects using this chart, based on the presence of multiple risk factors with visceral fat accumulation. On these conditions, health education "Hokenshido" program was provided by group and/or individual counseling. Public health nurse and dietitian interviewed and counseled the subjects about their pattern of meal, intake of alcohol, and habit of exercise. Through these processes, the guided subjects could determine the problematic habits which should be altered.

The number of subjects who received individual "Hokenshido" were 429 (13.5%) in year 2003, and 123 (3.9%) in year 2004. In particular, the subjects who could not improve their habit in the initial term were encouraged to repeatedly receive the group and individual lecture. The subjects considered already at high risk for CVD and chronic kidney diseases were referred to consult a cardiologist, neurologist, or nephrologist. Such subjects were continuously on the program to enhance the alteration of their problematic habits.

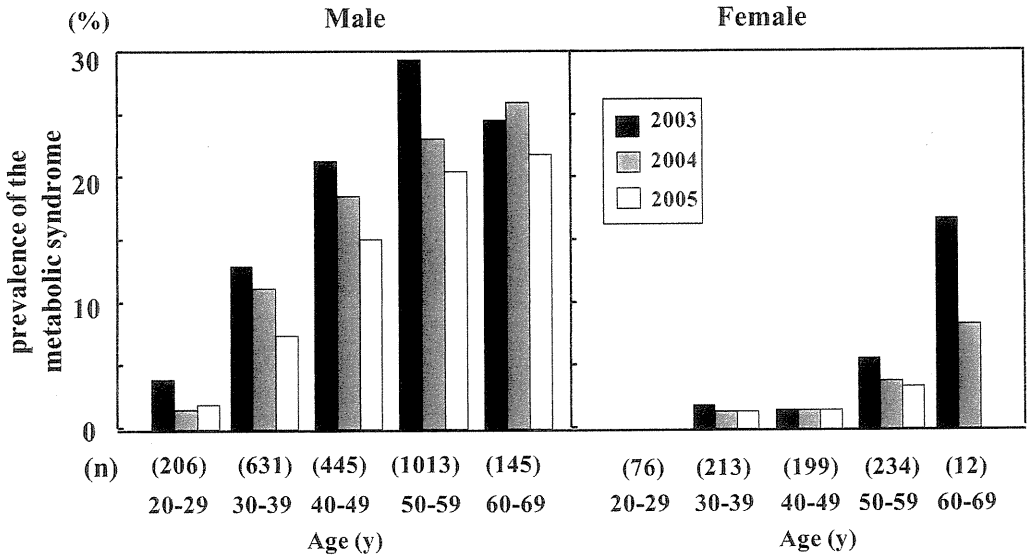

Figure 2. **Age-related prevalence of the metabolic syndrome from year 2003 to year 2005. Male (n=2,440), female (n=734). Kruskal Wallis test with a Scheffe's test.**

Table 2. **Change in Waist Circumferences**

		n	Waist circumference, cm			p
			year 2003	year 2004	year 2005	
Male	All	2440	84.9 ± 8.3	84.1 ± 8.4	83.3 ± 8.3	< 0.0001
	'03MS (+)	508	92.8 ± 6.7	91.5 ± 7.6	90.3 ± 7.4	< 0.0001
	'03MS (-)	1932	82.8 ± 7.4	82.1 ± 7.5	81.5 ± 7.5	< 0.0001
Female	All	734	78.2 ± 10.0	76.2 ± 9.4	76.7 ± 9.8	< 0.001
	'03MS (+)	22	98.3 ± 5.5	93.5 ± 6.6	94.4 ± 6.8	< 0.05
	'03MS (-)	712	77.6 ± 9.4	75.7 ± 9.0	76.2 ± 9.3	< 0.001

Data are means±SD.
'03MS (+), with the metabolic syndrome at baseline; '03MS (-), without the metabolic syndrome at baseline.
Kruskal-Wallist test with a Scheffe's test

Stastical analysis

The comparison of prevalence of the metabolic syndrome and risk factors in the 3 year period were analyzed by Kruskal Wallis test with a Scheffe's test. The statistical significance of the differences in the waist circumferences in 3 years were also analyzed by Kruskal Wallis test with a Scheffe's test. All statistical analyses were performed with StatView-J 5.0 (SAS Inc.).

Results

Age-related prevalence of the metabolic syndrome increased from the age of 30 years and was the highest in the 50-59 year age group in males and increased after the age of 50 years in females (Fig. 2). After initiating measurement of waist circumference in annual health checkup, use of "Where am I?" chart, and "Hokenshido", the prevalence decreased among males aged 30-39 years, 40-49 years, and 50-59 years ($p<0.01$), and among females aged 50-59 years, and 60-69 years during the 3-year period of this study.

The prevalence of the metabolic syndrome in 2003, 2004 and 2005 decreased in males (20.8%, 17.2%, 14.4%, $p<0.001$) and females (3.0%, 2.2%, 1.9%, $p=0.359$). Decreased prevalence of the metabolic syndrome in males was associated with significant reductions in the prevalence of abdominal obesity, dyslipidemia, and hypertension ($p<0.0001$). Among subjects with metabolic syndrome at baseline, the number of subjects with metabolic syndrome significantly decreased in males (508, 287, 247, $p<0.0001$) and females (22, 8, 6, $p<0.0001$), respectively.

Significant reductions of waist circumference were seen in males and females (Table 2). Mean waist loss was 1.6 cm in males ($p<0.0001$) and 1.5 cm in females ($p<0.001$). Among subjects with metabolic syndrome at baseline, the mean waist loss was 2.5 cm in males ($p<0.0001$) and 3.9 cm in females ($p<0.05$).

To be noted, during the 3-year period of this study, no fatal atherosclerotic vascular events were recorded.

Discussion

In the present study, we demonstrated that 1) after initiating measurement of waist circumference in annual health

checkup, use of "Where am I?" chart, and "Hokenshido" the prevalence of metabolic syndrome decreased with reductions in risk factors in males and females, 2) significant reductions of waist circumference were seen in males and females, 3) especially among males and females with the metabolic syndrome at baseline, the respective prevalence decreased markedly, and 4) fatal atherosclerotic vascular events were not recorded during the 3-year study period.

Based on the National Nutrition Survey in Japan, the rate of male obesity has been increasing. In this sense, the national campaign to improve the health of all Japanese people, called Kenko (Health) 21st, has not been fully successful. In the current study and program for the city employees, measurement of waist circumference and understanding of "Where am I?" chart seemed to be quite helpful to perceive their health conditions and reconsider the problematic habit. Through "Hokenshido", the guided subjects recognized a problem in their own lifestyle and attempted to reduce visceral fat as a goal to maintain a healthy life. In our Amagasaki Visceral Fat Study (8-17), we reported that the decrease in visceral fat was correlated with the decrease in the number of metabolic risk factors in the general male population (8).

Regarding the lack of fatal CVD events during the three-year study period, improvements of risk factors and possibly also the improvements of adipocytokine dysregulation such as hypoadiponectinemia might stabilize arterial plaque.

A limitation of this study is that majority of blood samples were nonfasting. To enhance annual health checkup for as many employees, such blood sampling policy, either fasting or nonfasting, is allowed by the employer in many work places in Japan. Data were evaluated according to the criteria described in Materials and Methods, dependent on individual fasting or non-fasting conditions. Furthermore subjects with one or two risks without obesity should be also followed-up closely. In this study, 180 (5.7%), 446 (14.1%), and 162 (5.1%) individuals were under treatment for dyslipidemia, hypertension, or diabetes, respectively, in year 2005.

Collectively, regular health checkups and "Hokenshido" program, which is based on the concept that visceral fat accumulation causes metabolic syndrome, effectively reduced the prevalence of the metabolic syndrome and various risk factors, which might lead to the prevention of CVD.

The authors state that they have no Conflict of Interest (COI).

Acknowledgement

We gratefully acknowledge Sachiko Morita (Amagasaki City Office) for research and comment, and Dr.Tomohiro Onda and Mitsuhiro Katashima (Kao Corporation) for technical assistance and comment.

References

1. Alberti KG, Zimmet P, Shaw J; IDF Epidemiology Task Force Consensus Group. The metabolic syndrome: A new worldwide definition. Lancet **366**: 1059-1062, 2005.
2. Fujioka S, Matsuzawa Y, Tokunaga K, Tarui S. Contribution of intra-abdominal fat accumulation to the impairment of glucose and lipid metabolism in human obesity. Metabolism **36**: 54-59, 1987.
3. Kanai H, Matsuzawa Y, Kotani K, et al. Close correlation of intra-abdominal fat accumulation to hypertension in obese women. Hypertension **16**: 484-490, 1990.
4. Nakamura T, Tokunaga K, Shimomura I, et al. Contribution of visceral fat accumulation to the development of coronary artery disease in non-obese men. Atherosclerosis **107**: 239-246, 1994.
5. Grundy SM, Cleeman JI, Merz CN, et al. Implication of recent clinical trials for the National Cholesterol Education Program Adult Treatment Panel III guidelines. Circulation **110**: 227-239, 2004.
6. Despres JP, Lemieux I. Abdominal obesity and metabolic syndrome. Nature **444**: 881-887, 2006.
7. Grundy SM, Cleeman JI, Daniels SR, et al. Diagnosis and management of the metabolic syndrome: An American Heart Association/National Heart, Lung, and Blood Institute Scientific Statement. Circulation **112**: 2735-2752, 2005.
8. Okauchi Y, Nishizawa H, Funahashi T, et al. Reduction of visceral fat is associated with decrease in the number of metabolic risk factors in Japanese men. Diabetes Care **30**: 2392-2394, 2007.
9. Tamba S, Nishizawa H, Funahashi T, et al. Relationship between the serum uric acid level, visceral fat accumulation and serum adiponectin concentration in Japanese men. Intern Med **47**: 1175-1180, 2008.
10. Akita EF, Okita K, Okauchi Y, et al. Impaired early insulin secretion in Japanese type 2 diabetes with metabolic syndrome. Diabetes Res Clin Pract **79**: 482-489, 2008.
11. Okauchi Y, Kishida K, Funahashi T, et al. Changes in serum adiponectin concentrations correlate with changes in BMI, waist circumference, and estimated visceral fat area in middle-aged general population. Diabetes Care **32**: e122, 2009.
12. Kamada Y, Nakamura T, Funahashi T, et al. Visceral obesity and hypoadiponectinemia are significant determinants of hepatic dysfunction: An epidemiologic study of 3827 Japanese subjects. J Clin Gastroenterol **43**: 995-1000, 2009.
13. Tamba S, Nakatsuji H, Kishida K, et al. Relationship between visceral fat accumulation and urinary albumin-creatinine ratio in middle-aged Japanese men. Atherosclerosis **211**: 601-605, 2010.
14. Nakatsuji H, Kishida K, Funahashi T, et al. One-year reductions in body weight and blood pressure, but not in visceral fat accumulation and adiponectin, improve urinary albumin-to-creatinine ratio in middle-aged Japanese men. Diabetes Care **33**: e110-e111, 2010.
15. Okauchi Y, Kishida K, Funahashi T, et al. Absolute value of bioelectrical impedance analysis-measured visceral fat area with obesity-related cardiovascular risk factors in Japanese workers. J Atheroscler Thromb **17**: 1237-1245, 2010.
16. Okauchi Y, Kishida K, Funahashi T, et al. 4-year follow-up of cardiovascular events and changes in visceral fat accumulation after health promotion program in the Amagasaki Visceral Fat Study. Atherosclerosis **212**: 698-700, 2010.
17. Akita EF, Iwahashi H, Okauchi Y, et al. Predictors of deterioration of glucose tolerance and effects of lifestyle intervention aimed at reducing visceral fat in normal glucose tolerance subjects with abdominal obesity. J Diabetes Invest **2**: 218-224, 2011.
18. Tokunaga K, Matsuzawa Y, Ishikawa K, Tarui S. A novel technique for the determination of body fat by computed tomography. Int J Obes **7**: 437-445, 1983.
19. Matsuzawa Y. Metabolic syndrome-definition and diagnostic criteria in Japan. J Atheroscler Thromb **12**: 301, 2005.
20. Eberly LE, Stamler J, Neaton JD: Multiple Risk Factor Intervention Trial Research Group. Relation of triglyceride levels, fasting and nonfasting, to fatal and nonfatal coronary heart disease. Arch Intern Med **163**: 1077-1083, 2003.
21. Ahmad J, Hameed B, Das G, Siddiqui M, Ahmad I. Postprandial

hypertriglyceridemia and carotid intima-media thickness in north Indian type 2 diabetic subjects. Diabetes Res Clin Pract **69**: 142-150, 2005.

22. American Diabetes Association. Clinical practice recommendations 2000: screening for type 2 diabetes. Diabetes Care **23**: S20-S23, 2000.

Deficit of tRNA^{Lys} modification by Cdkal1 causes the development of type 2 diabetes in mice

Fan-Yan Wei,[1] Takeo Suzuki,[2] Sayaka Watanabe,[1] Satoshi Kimura,[2] Taku Kaitsuka,[1] Atsushi Fujimura,[3] Hideki Matsui,[3] Mohamed Atta,[4] Hiroyuki Michiue,[3] Marc Fontecave,[4] Kazuya Yamagata,[5] Tsutomu Suzuki,[2] and Kazuhito Tomizawa[1]

[1]Department of Molecular Physiology, Faculty of Life Sciences, Kumamoto University, Kumamoto, Japan. [2]Department of Chemistry and Biotechnology, School of Engineering, The University of Tokyo, Tokyo, Japan. [3]Department of Physiology, Okayama University Graduate School of Medicine, Dentistry and Pharmaceutical Sciences, Okayama, Japan. [4]Institut de Recherches en Technologie et Sciences pour le Vivant IRTSV-LCBM, UMR 5249, CEA/CNRS/UJF, CEA-Grenoble, Grenoble, France. [5]Department of Medical Biochemistry, Faculty of Life Sciences, Kumamoto University, Kumamoto, Japan.

The worldwide prevalence of type 2 diabetes (T2D), which is caused by a combination of environmental and genetic factors, is increasing. With regard to genetic factors, variations in the gene encoding Cdk5 regulatory associated protein 1–like 1 (Cdkal1) have been associated with an impaired insulin response and increased risk of T2D across different ethnic populations, but the molecular function of this protein has not been characterized. Here, we show that Cdkal1 is a mammalian methylthiotransferase that biosynthesizes 2-methylthio-N^6-threonylcarbamoyladenosine (ms^2t^6A) in tRNA^{Lys}(UUU) and that it is required for the accurate translation of AAA and AAG codons. Mice with pancreatic β cell–specific KO of Cdkal1 (referred to herein as β cell KO mice) showed pancreatic islet hypertrophy, a decrease in insulin secretion, and impaired blood glucose control. In Cdkal1-deficient β cells, misreading of Lys codon in proinsulin occurred, resulting in a reduction of glucose-stimulated proinsulin synthesis. Moreover, expression of ER stress–related genes was upregulated in these cells, and abnormally structured ER was observed. Further, the β cell KO mice were hypersensitive to high fat diet–induced ER stress. These findings suggest that glucose-stimulated translation of proinsulin may require fully modified tRNA^{Lys}(UUU), which could potentially explain the molecular pathogenesis of T2D in patients carrying *cdkal1* risk alleles.

Introduction

Type 2 diabetes (T2D) is caused by a combination of genetic and environmental factors. Recent advances in whole-genome association studies have identified a number of genetic variations associated with T2D (1–4). The Cdk5 regulatory associated protein 1–like 1 (*cdkal1*) gene is one of the most reproducible risk genes in T2D across different ethnic populations (5). Variations in *cdkal1* have been associated with impaired insulin secretion and increased risk of T2D (6–8). Although there is increasing evidence associating single nucleotide polymorphisms in *cdkal1* with T2D, the molecular function of Cdkal1 is unknown.

We recently identified Cdkal1 as a member of the methylthiotransferase (MTTase) family, a subfamily of the radical S-adenosylmethionine (SAM) superfamily (9). The MTTase family utilizes SAM and [4Fe-4S] clusters to catalyze the methylthiolation of various substrates. For instance, MiaB, a bacterial MTTase protein, catalyzes the methylthiolation of N^6-isopentenyladenosine (i^6A) to generate 2-methylthio-N^6-isopentenyladenosine (ms^2i^6A) at position 37 (A^{37}), 3′ adjacent to the anticodon in some tRNAs (10, 11). This hypermodification of A^{37} is essential for the efficient and accurate translation of cognate codons by the ribosome (12, 13). We have shown that Cdkal1 (and its bacterial homolog YqeV) catalyze the methylthiolation of N^6-threonyl carbamoyl adenosine (t^6A) to synthesize 2-methylthio-N^6-threonyl carbamoyl adenosine (ms^2t^6A) for tRNA in bacteria (9). However, the enzymatic characteristics of Cdkal1 in mammalian cells and its relevance to T2D are completely unknown. By using pancreatic β cell–specific Cdkal1 KO mice (referred to herein as β cell KO mice), we show that Cdkal1 has critical roles in the quality control of protein translation and is relevant to T2D.

Results

Cdkal1 catalyzes ms^2t^6A modification of mammalian tRNA^{Lys}(UUU). To determine the biochemical function of Cdkal1 in mammalian cells and its relevance to T2D, we used mass spectrometric analysis to examine modified bases in total RNA from MIN6 cells, a pancreatic β cell–derived insulinoma cell line, and HeLa cells, a human-derived cell line (Figure 1B). As expected, the proton adduct ms^2t^6A (m/z 459) could be clearly detected along with t^6A (m/z 413) in both cell types (Figure 1B). In addition, we also detected ms^2t^6A in total RNA from various mouse tissues (Supplemental Figure 1; supplemental material available online with this article; doi:10.1172/JCI58056DS1). To investigate whether Cdkal1 was involved in the ms^2t^6A modification, we examined total RNA isolated from the pancreas of WT and *Cdkal1*$^{-/-}$ mice. The ms^2t^6A modification was detected only in the WT mice but not in the *Cdkal1*$^{-/-}$ mice (Figure 1C). These results suggest that Cdkal1 only catalyzes the ms^2t^6A modification in mammalian cells. Because ms^2t^6A is present at position 37 of tRNA^{Lys} in *Bacillus subtilis* (14, 15), we isolated 2 species of tRNA^{Lys} (tRNA^{Lys}[UUU] [Figure 1A] and tRNA^{Lys}[CUU] [Supplemental Figure 2A]) from mouse livers and performed an RNA

Authorship note: Takeo Suzuki and Sayaka Watanabe contributed equally to this work.

Conflict of interest: The authors have declared that no conflict of interest exists.

Citation for this article: *J Clin Invest.* 2011;121(9):3598–3608. doi:10.1172/JCI58056.

fragment analysis. ms^2t^6A was specifically found at position 37 of $tRNA^{Lys}$(UUU) in WT liver (Figure 1D), whereas $tRNA^{Lys}$(CUU) bore t^6A at position 37 (Supplemental Figure 2B). As no fragment containing t^6A was detected in $tRNA^{Lys}$(UUU) of WT liver, the methylthio modification appeared to be introduced universally (Figure 1D). When the nucleosides from the flow-through fraction after the isolation of $tRNA^{Lys}$(UUU) were analyzed, no ms^2t^6A could be detected (Supplemental Figure 3), suggesting that ms^2t^6A is a modification specific to $tRNA^{Lys}$(UUU). In contrast, the ms^2t^6A-containing fragment (m/z 1172.16) was completely replaced with a t^6A-containing fragment (m/z 1126.17) in $tRNA^{Lys}$(UUU) isolated from livers of *Cdkal1*$^{-/-}$ mice (Figure 1D). These results demonstrate that mouse Cdkal1 is a methylthiolase that converts t^6A to ms^2t^6A in $tRNA^{Lys}$(UUU).

The ms^2t^6A modification is required for decoding fidelity. The 2-methylthio modification ms^2i^6A is important for preventing the misreading and frame-shifting of cognate codons during protein translation in bacteria (12–14). These observations prompted us to speculate that the 2-methylthio modification ms^2t^6A in $tRNA^{Lys}$(UUU) is also required for translational accuracy. To examine whether the ms^2t^6A modification prevents either the frame-shifting or misreading of $tRNA^{Lys}$(UUU)'s cognate codons (AAA and AAG), we utilized a dual luciferase-based reporter assay in WT *B. subtilis* and *yqeV*-deficient *B. subtilis* (Δ*yqeV*), which lacks the ms^2t^6A modification (Supplemental Figure 4A, Figure 1E, and ref. 16). Because Lys529 in *firefly* luciferase is essential for enzymatic activity, the misreading or frameshifting of this codon would result in a loss of *firefly* luciferase activity (17, 18). Two constructs in which Lys529 is encoded by AAA or AAG codons were introduced into WT and Δ*yqeV* strains, and relative *firefly* luciferase activity was measured (Figure 1E). In the Δ*yqeV* strain under noninducible conditions (–IPTG), a specific reduction in *firefly* luciferase activity was observed with the AAA construct, but not with the AAG construct (Figure 1E). Under inducible conditions (+IPTG), a marked reduction in *firefly* luciferase activity was observed with both constructs in the Δ*yqeV* strain, and an even greater reduction in activity was observed with the AAG construct (Figure 1E), although the IPTG-induced protein level of the *renilla-firefly* fusion protein was the same in the WT and Δ*yqeV* strains (Figure 1F). We next determined whether the 2-methylthio modification ms^2t^6A is involved in the reading frame maintenance of the relevant codons. We employed constructs that fused *Renilla* and *firefly* luciferases separated by a short sequence containing a +1 frameshift site (Supplemental Figure 4B). We observed no significant frameshift activity of either construct in the Δ*yqeV* strain as compared with the WT strain. These results suggest that the 2-methylthio modification ms^2t^6A in $tRNA^{Lys}$(UUU) is important for preventing the misreading of its cognate codons, especially when the rate of translation is relatively high.

Cdkal1 is an ER-localizing protein that is functionally dissociated with Cdk5/p35. Cdkal1 was ubiquitously expressed in mouse tissues through all the developmental stages and was especially abundant in the heart, kidney, and pancreas (Supplemental Figure 5). To investigate the subcellular distribution of Cdkal1, HEK293 and MIN6 cells were transfected with EGFP-Cdkal1 and ER-tracker. EGFP-Cdkal1 colocalized with ER-tracker (Figure 2A). Moreover, Cdkal1 was also colocalized with endogenous Bip, an ER protein (Figure 2B). Cdkal1 has 3 unique domains, a radical SAM domain, a TRAM domain, and a hydrophobic domain (Figure 2C). Both the radical SAM domain (a catalytic domain) and the TRAM domain (a potential tRNA-binding domain) are conserved among mammals and bacteria (9). In contrast, the hydrophobic domain at the C terminus exists only in mammalian Cdkal1 (9). This hydrophobic domain was determined to carry the ER-localization signal because deletion of this domain disrupted ER localization (Figure 2D). Furthermore, endogenous Cdkal1 was detected in the rough ER fraction purified from mouse liver (Supplemental Figure 6). The ER localization was finally confirmed by immunoelectron microscopic examination in EGFP-Cdkal1–transfected MIN6 cells (Figure 2E).

We previously reported that Cdk5 regulates insulin secretion in pancreatic β cells (19). Cdkal1 may function through interaction with a Cdk5 regulatory subunit, p35, as Cdk5rap1, an amino acid homolog of Cdkal1, interacts with p35 and inhibits Cdk5 activity (20, 21). However, Cdkal1 neither interacted with p35 in HEK293 cells overexpressing p35 nor inhibited Cdk5 activity in vitro (Supplemental Figure 7), suggesting that the molecular function of Cdkal1 in β cells is independent of the pathway in which Cdk5/p35 participates.

Cdkal1 deficiency in β cells causes glucose intolerance. To investigate the physiological functions of Cdkal1 in pancreatic β cells, β cell–specific Cdkal1-deficient mice (β cell KO) were generated by crossing transgenic mice in which exon 5 of *cdkal1* was floxed by the LoxP sequence with transgenic mice in which Cre recombinase was regulated under the control of the rat insulin promoter (Supplemental Figure 8A). Exon 5 of *cdkal1* was deleted in the pancreatic islets of β cell KO mice, but not the other tissues of the β cell KO mice, (Supplemental Figure 8B). Cdkal1 protein expression was faint in the islets of β cell KO mice compared with that in the islets of littermate control mice (Flox) (Figure 3A). In contrast, the same level of Cdkal1 was observed in kidney of Flox mice and β cell KO mice (Figure 3A). The β cell KO mice showed normal development (Figure 3B). Immunohistochemical analyses revealed no obvious morphological abnormalities in α or β cells in the pancreatic islets of β cell KO mice relative to Flox mice (Figure 3C). However, we noticed that KO islets were larger than Flox islets, and we performed a detailed analysis to investigate islet area. We divided the islets into 3 groups: small islets (0–5,000 μm^2), medium islets (5,001–10,000 μm^2), and large islets (>10,000 μm^2), and we calculated the relative abundance of each group. In β cell KO mice, the number of small islets was significantly lower than in Flox mice, and the number of large islets was significantly greater (Figure 3D). Because there was no difference in total islet number between β cell KO and Flox mice (data not shown), pancreatic islets in β cell KO mice may be able to lapse into a hypertrophic condition.

Because insulin secretion is impaired in patients with variants of the *cdkal1* gene (6–8), the mice were given an intraperitoneal glucose tolerance test (IPGTT). The β cell KO mice showed glucose intolerance compared with the Flox mice at 5 and 10 weeks after birth (Figure 3E). Moreover, plasma insulin levels 15 minutes after the glucose challenge were significantly lower in the β cell KO mice (Figure 3F). We also investigated insulin secretion in islets isolated from Flox and β cell KO mice. After 16.7 mM glucose stimulation, the insulin level was significantly lower in β cell KO mice than in Flox mice (Figure 3G). Because patients with variants of the *cdkal1* gene showed a specific impairment of first-phase insulin secretion (6), we investigated whether a deficiency of Cdkal1 has any effect on the biphasic secretion of insulin. We examined glucose-stimulated insulin secretion in perifused islets isolated from Flox and β cell KO mice. The KO islets showed impaired first-phase, but not second-phase, insulin secretion upon stimulation with 16.7 mM glucose compared with the Flox islets (Figure 3H). Furthermore, we also

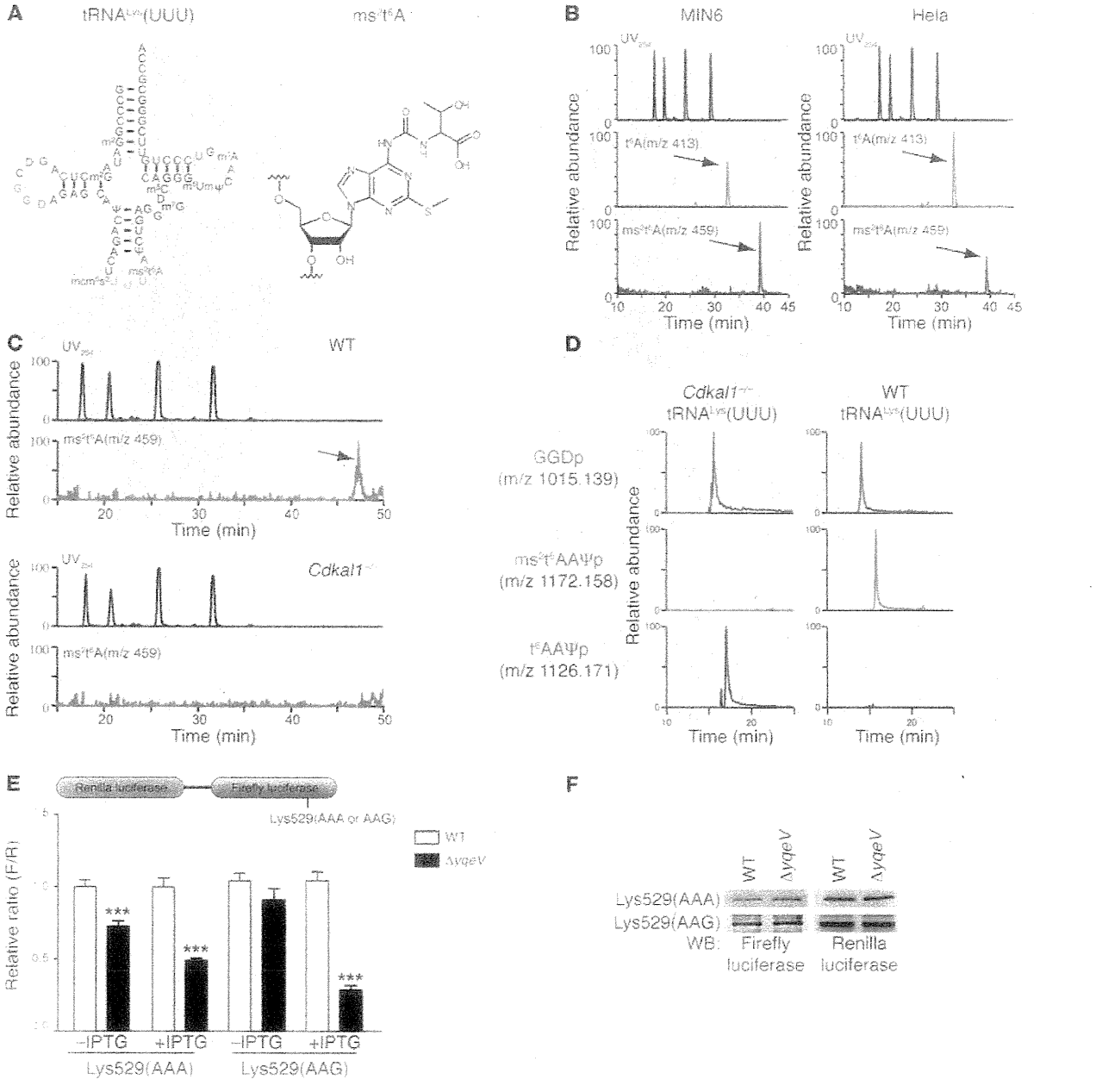

Figure 1

Methylthiolation of tRNA^{Lys}(UUU) by Cdkal1 controls the decoding accuracy of the lysine codon. (**A**) The molecular structure of tRNA^{Lys}(UUU) and ms^{2}t^{6}A. (**B**) Results of a mass spectrometric analysis of the ms^{2}t^{6}A modification of tRNA in MIN6 and HeLa cells. The upper panels show the UV trace, and the middle and lower panels show the mass chromatograms for detecting t^{6}A (m/z 413, arrow) and ms^{2}t^{6}A (m/z 459, arrow), respectively. (**C**) Results of a mass spectrometric analysis of the ms^{2}t^{6}A modification of tRNA isolated from the pancreas of *Cdkal1*$^{-/-}$ and WT mice. The arrow indicates ms^{2}t^{6}A (m/z 459). (**D**) Modification of tRNA^{Lys}(UUU) isolated from the liver of *Cdkal1*$^{-/-}$ and WT mice. The upper panels show mass chromatograms of GGDp fragments in tRNA^{Lys}(UUU). The middle and lower panels show mass chromatograms of ms2t6AAΨp fragments and t6AAΨp fragments, respectively. (**E**) WT and Δ*yqeV* cells were transformed with a reporter plasmid in which both Renilla renilla and firefly luciferases are cloned with the lac promoter (upper panel). Relative activity was determined by normalizing firefly luciferase intensity to renilla luciferase intensity (F/R, lower panel). Data are presented as the mean ± SEM. and asterisks indicate statistical significance determined by Student's *t* test. $^{***}P < 0.001$; $n = 4$. (**F**) The expression level of the fusion protein of firefly and renilla luciferase after IPTG treatment induction was determined in WT and Δ*yqeV* cells (**E**) by Western blot.

investigated insulin secretion in Flox and β cell KO mice under normal feeding conditions. The mice were fasted overnight and then re-fed for 1.5 hours. Plasma insulin levels in the fasting condition and postprandial condition were determined (Figure 3I). There was a significant decrease in postprandial insulin secretion in β cell KO mice when compared with Flox mice. These results suggest that Cdkal1 deficiency in pancreatic β cells impairs glucose-stimulated insulin secretion and thus induces glucose intolerance.

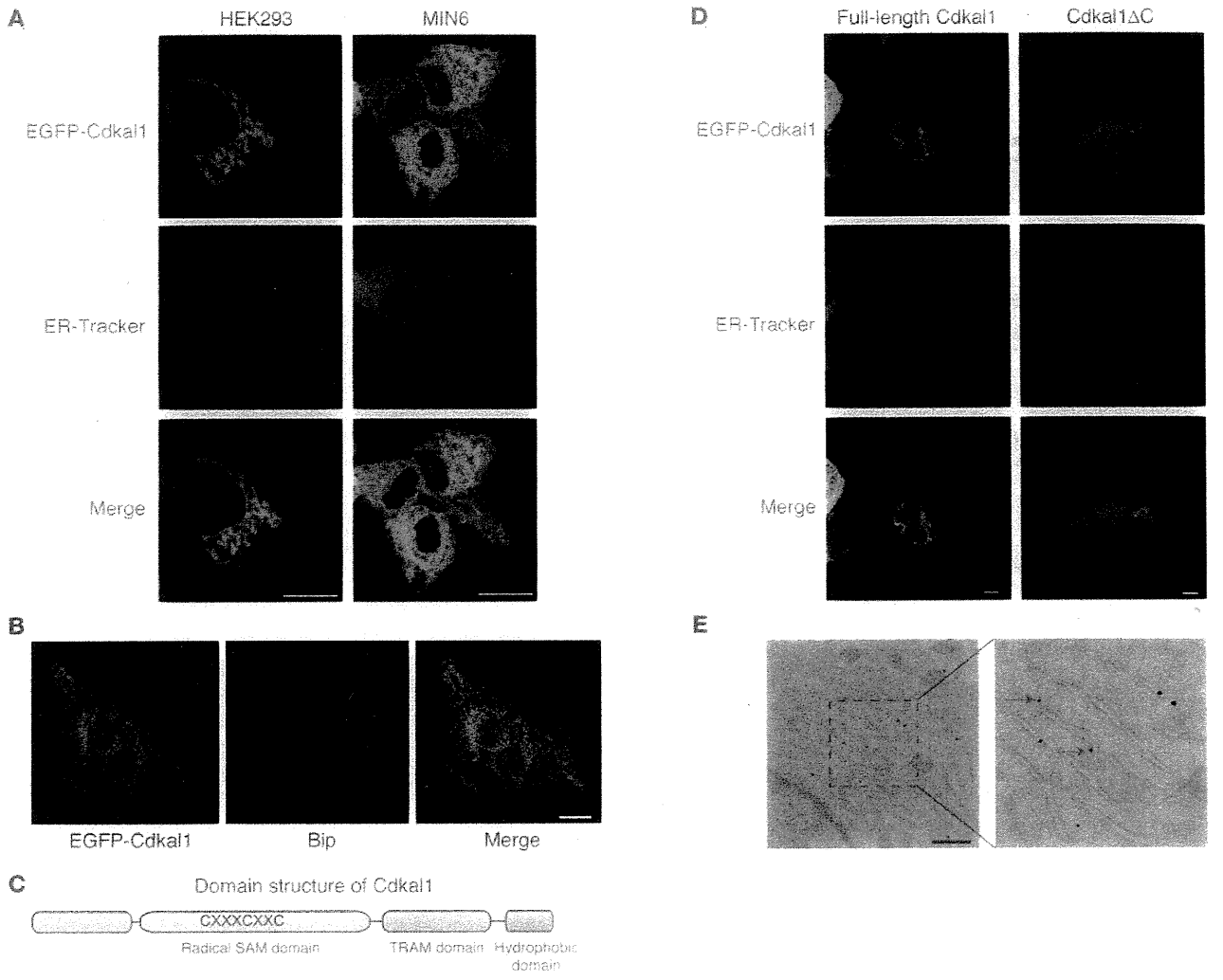

Figure 2

Cdkal1 localizes on ER through its hydrophobic domain. (**A**) Colocalization of overexpressed Cdkal1-EGFP (green) and ER-tracker (red) on ER in HEK293 cells and MIN6 cell. Scale bars: 10 μm. (**B**) Colocalization of overexpressed Cdkal1-EGFP (green) with endogenous Bip in HEK293 cells. Scale bar: 10 μm. (**C**) The domain structure of Cdkal1 protein. (**D**) EGFP-tagged full-length Cdkal1 or Cdkal1 with truncation of C terminus hydrophobic domain (Cdkal1ΔC) was transfected in HeLa cells together with ER-tracker. Localization of full-length Cdkal1 or Cdkal1ΔC was visualized using confocal microscope. Scale bars: 10 μm. (**E**) MIN6 cells were transfected with Cdkal1-EGFP, and the localization of Cdkal1 was determined by immunoelectronic microscopic examination. Arrows indicate EGFP-Cdkal1 signal on ER. Scale bar: 0.5 μm.

Cdkal1 deficiency induces aberrant proinsulin synthesis. Given the molecular function of Cdkal1 in *B. subtilis* (Figure 1), we speculated that Cdkal1 deficiency in pancreatic β cells decreases the decoding fidelity in lysine codon due to insufficient modification in $tRNA^{Lys}(UUU)$. The Lys residue is particularly important for processing proinsulin to generate mature insulin and C-peptide because 1 of the 2 Lys residues in human proinsulin is located at the cleavage site between the C-peptide and A chain of insulin. Thus, misreading of Lys codon in proinsulin by insufficiently modified $tRNA^{Lys}(UUU)$ might result in aberrant processing of (pro)insulin and subsequent glucose intolerance. To investigate misreading of Lys codon in Cdkal1-deficient β cells, pancreatic islets isolated from both β cell KO and Flox mice were labeled with both ^{14}C-lysine and ^{3}H-leucine. If misreading of Lys codon occurs in Cdkal1-deficient β cells, we would observe a change in the ratio of incorporation of ^{14}C-lysine to ^{3}H-leucine in (pro)insulin when compared with the incorporation ratio in Flox β cells. As expected, there was a significant decrease of relative incorporation of ^{14}C-lysine in (pro)insulin in Cdkal1-deficient β cells when compared with Flox β cells (KO: 0.82 ± 0.007 versus Flox: 1.0 ± 0.01, $P = 0.0004$; Figure 4A). Since misreading of Lys codon in proinsulin might cause aberrant processing, we investigated the C-peptide content, which indicates proper processing of proinsulin, in the pancreas of β cell KO and Flox mice. The C-peptide content in β cell KO pancreas was significantly lower than C-peptide content in Flox pancreas (β cell KO: 12.4 ± 1.41 ng/mg protein versus Flox: 22.4 ± 3.29 ng/ mg protein. $P = 0.0429$; Figure 4B). Accordingly, plasma C-peptide levels were significantly lower in β cell KO mice than in Flox mice (Figure 4C). Pancreatic sections were also immunostained with anti–C-peptide antibodies. Consistent with the reduction in C-peptide levels in β cell KO mice, the intensity of C-peptide stain-

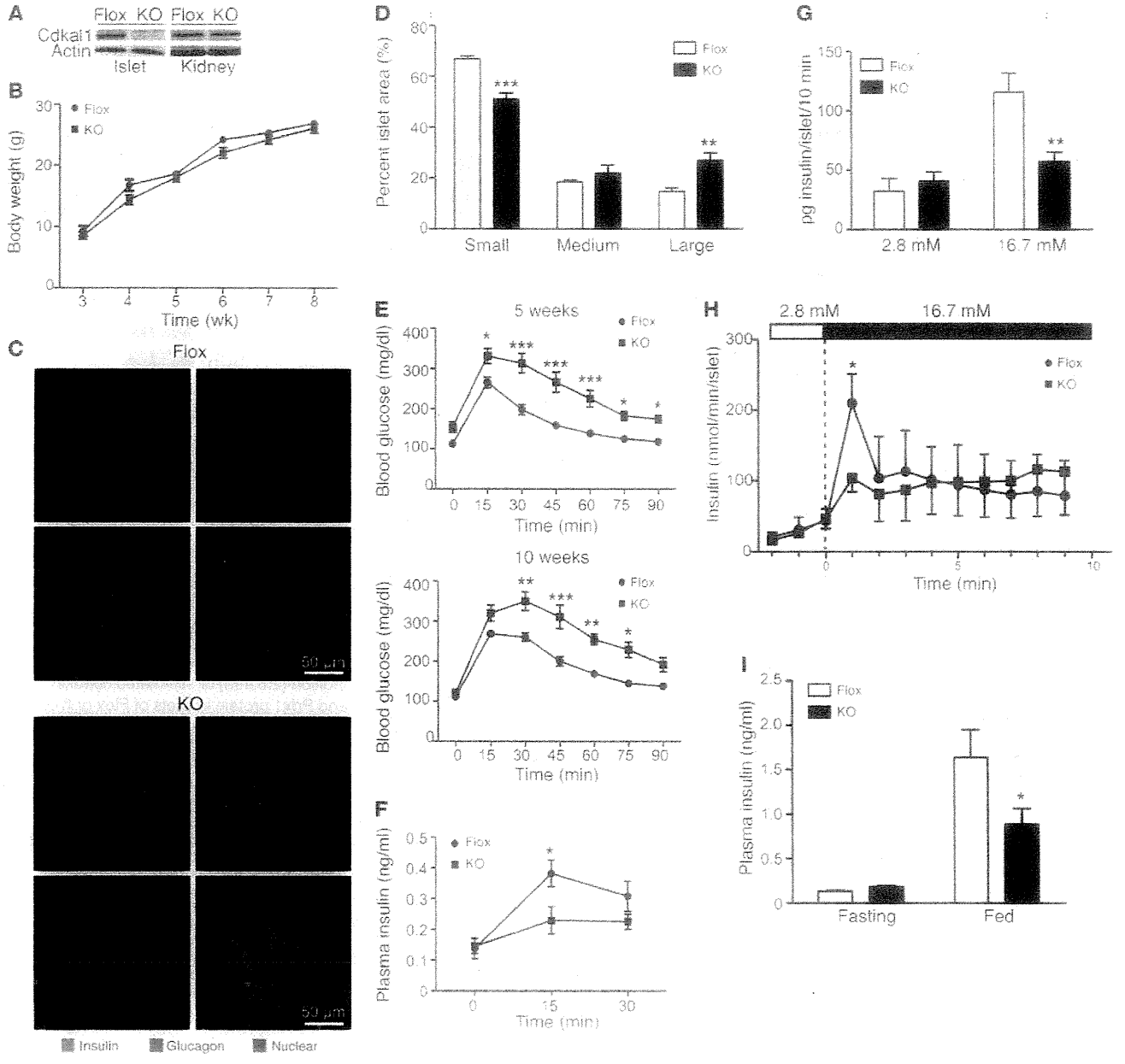

Figure 3

Conditional deletion of the *Cdkal1* gene causes glucose intolerance. (**A**) Conditional deletion of *Cdkal1* in pancreatic islets in β cell KO (KO) mouse. (**B**) Comparison of the body weights of β cell KO and Flox mice. (**C**) Pancreatic sections obtained from β cell KO and Flox mice at 5 weeks of age were immunostained with anti-insulin (red) and anti-glucagon (green) antibodies. Nuclei were counterstained with DAPI. (**D**) Comparison of relative islet area in pancreas of β cell KO and Flox mice. Area of 529 islets from 3 Flox mice and 572 islets from 3 β cell KO mice were examined and classified into small, medium, and large islet area. The relative distribution of each islet area was compared between β cell KO and Flox. (**E**) Blood glucose during glucose tolerance test at 5 weeks (upper) and 10 weeks (lower). $n = 4–7$. (**F**) Plasma insulin levels during a glucose tolerance test at 15 weeks. $n = 10–11$. (**G**) Glucose-stimulated insulin secretion in islets ($n = 8$) isolated from β cell KO or Flox mice was determined. (**H**) Glucose-stimulated insulin secretion in perfused islets of Flox and β cell KO mice. $n = 4–5$. (**I**) Plasma insulin levels in Flox or β cell KO mice fasted for 14 hours and re-fed for 1.5 hours. $n = 7$. Significant difference was examined by repeated measure of 2-way ANOVA (**E** and **F**) or 2-way ANOVA (**D**, **G**, and **I**) followed by Bonferroni's post-test or Mann-Whitney *U* test. Data are presented as mean ± SEM. $^*P < 0.05$; $^{**}P < 0.01$; $^{***}P < 0.001$ versus Flox.

ing was apparently reduced in KO islets compared with Flox islets (Supplemental Figure 9A). Previous study using pancreatic β cell-specific transgenic mice overexpressing mutant eIF2α has shown that aberrant protein translation could impair the correct targeting of proinsulin (22). Therefore, subcellular localization of proinsulin was investigated in β cell KO mice. High magnification revealed that proinsulin was mainly confined to the perinuclear area and colocalized with C-peptide in the β cells of Flox mice. In contrast,

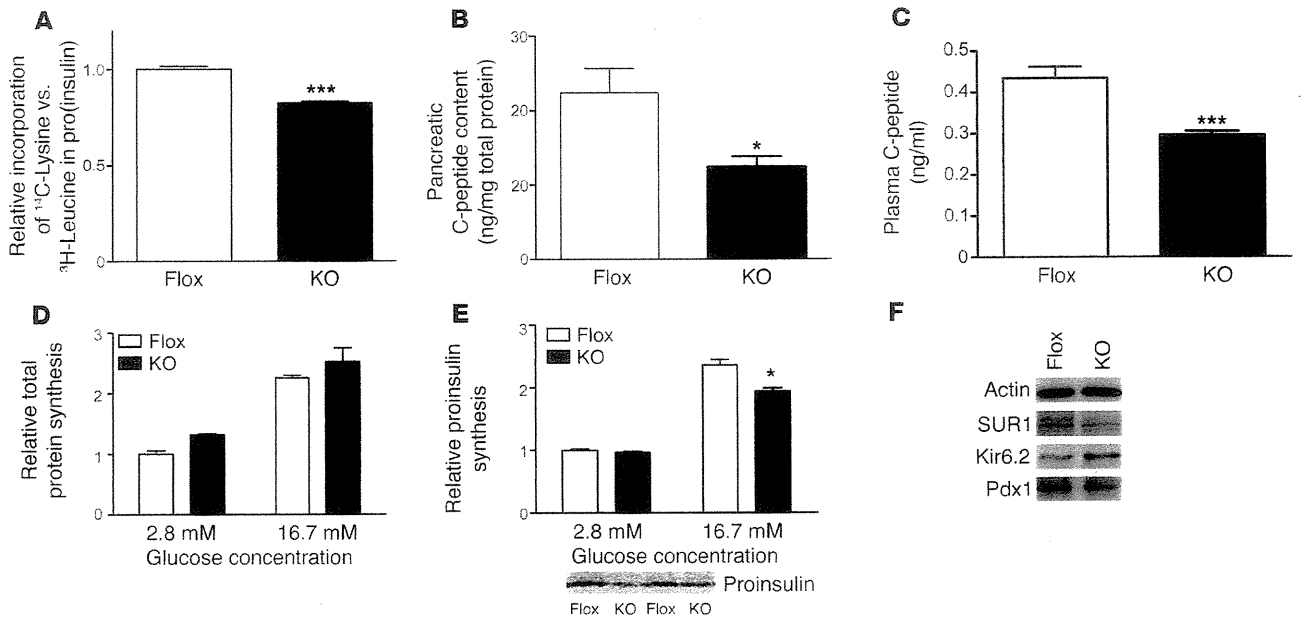

Figure 4

Aberrant insulin synthesis in the pancreatic β cells of β cell KO mice. (**A**) Relative incorporation of 14C-lysine to 3H-leucine in immunoprecipitated (pro)insulin in islets of β cell KO or Flox mice in KRB buffer containing 16.7 mM glucose for 1 hour. (**B**) Pancreatic C-peptide content of β cell KO or Flox mice was measured by ELISA, and value was normalized to total protein concentration. $n = 5–8$; $^*P < 0.05$ by Student's t test. (**C**) Plasma C-peptide concentrations in Flox and β cell KO mice fasted for 7 hours. $n = 10$. $^{***}P < 0.001$ by Student's t test. (**D**) Relative total protein synthesis under basal condition (2.8 mM) or stimulated condition (16.7 mM) was determined by normalizing 35S incorporation to the total protein concentration. $n = 4$; $^*P < 0.05$ by Student's t test. (**E**) Proinsulin synthesis in KO or Flox islets under basal condition (2.8 mM) or stimulated condition (16.7 mM) is shown in top panel. $n = 4$; $^*P < 0.05$ by Student's t test. (**F**) Expression of actin, SUR1, Kir6.2, and Pdx1 protein in islets of Flox or β cell KO mice determined by Western blotting. Results representative of 3 independent experiments are shown. All data are presented as mean ± SEM.

there were large aggregates of proinsulin-positive granules, which were not colocalized with C-peptide–positive granules in islets of β cell KO mice (Supplemental Figure 9B). These results suggest that Cdkal1 deficiency may cause abnormal proinsulin translation, which in turn leads to the impairment of both the processing and targeting of proinsulin.

In addition, we investigated the total protein synthesis level and proinsulin synthesis level in islets of β cell KO and Flox mice. Total protein synthesis in KO islets was not changed under either low- or high-glucose conditions (Figure 4D). There was no difference in proinsulin levels between KO islets and control islets under low-glucose conditions (Figure 4E). However, a significant decrease in proinsulin synthesis was observed in KO islets stimulated with high glucose compared with Flox islets (Figure 4E). A decrease in insulin synthesis was also observed in MIN6 cells transfected with siRNA targeting Cdkal1 (Supplemental Figure 10). To investigate whether Cdkal1 deficiency had any effect on the synthesis of other crucial β cell proteins, we examined the protein levels of Kir6.2, SUR1, and Pdx1. There were no obvious differences in protein levels between KO islets and Flox islets (Figure 4F). These results suggest that tRNA modification by Cdkal1 is crucial for translation fidelity and efficiency of proinsulin in pancreatic β cells.

Cdkal1 deficiency induces ER stress in β cells. Accumulation of unfolded or misfolded proteins in the ER lumen triggers stress response, which has been proposed to cause the dysfunction of pancreatic β cells (22–25). Notably, temporary or chronic imbalance in the protein synthesis environment can induce ER stress in β cells and subsequent glucose intolerance in vivo (22, 26, 27). To investigate whether aberrant proinsulin synthesis caused by Cdkal1 deficiency triggers stress responses in β cells, we examined the expression levels of a variety of genes essential for β cell function. There were no differences in the levels of insulin 1 or 2 mRNAs between KO and Flox islets (Figure 5A). Among pancreatic β cell marker genes, the mRNA levels of glucose transporter 2 (*Glut2*) were significantly reduced in KO islets (Figure 5B). Moreover, Glut2 was distributed diffusely in the cytoplasm of β cells in Cdkal1-deficient islets (Figure 5C). The decreased expression and abnormal localization of Glut2 correlate with ER stress (22). Therefore, the relative expression of ER stress–related genes was then examined in the pancreatic islets of β cell KO and Flox mice. Among all the stress-related genes, only the expression of spliced *Xbp1* was found to be elevated (Figure 5D). In addition, phospho-EIF2 levels were higher in KO islets than in Flox islets (Supplemental Figure 11). Furthermore, electron microscopy revealed distended ER, which indicates ER stress (27, 28), in pancreatic β cells from β cell KO mice but not from Flox mice (Figure 5E). These results suggest that *cdkal1* gene deficiency may induce an ER stress response and glucose intolerance.

Cdkal1 deficiency enhances susceptibility to high-fat diet stress. Environmental stress such as a high-fat diet (HFD) has a great impact on glucose metabolism. Interestingly, recent study has found the association of polymorphism in the *cdkal1* gene with the prevalence of metabolic syndrome in Japanese men (29). We therefore speculated that a HFD might induce profound glucose intolerance in β cell KO mice. To investigate the effect of an HFD, β cell KO and Flox mice

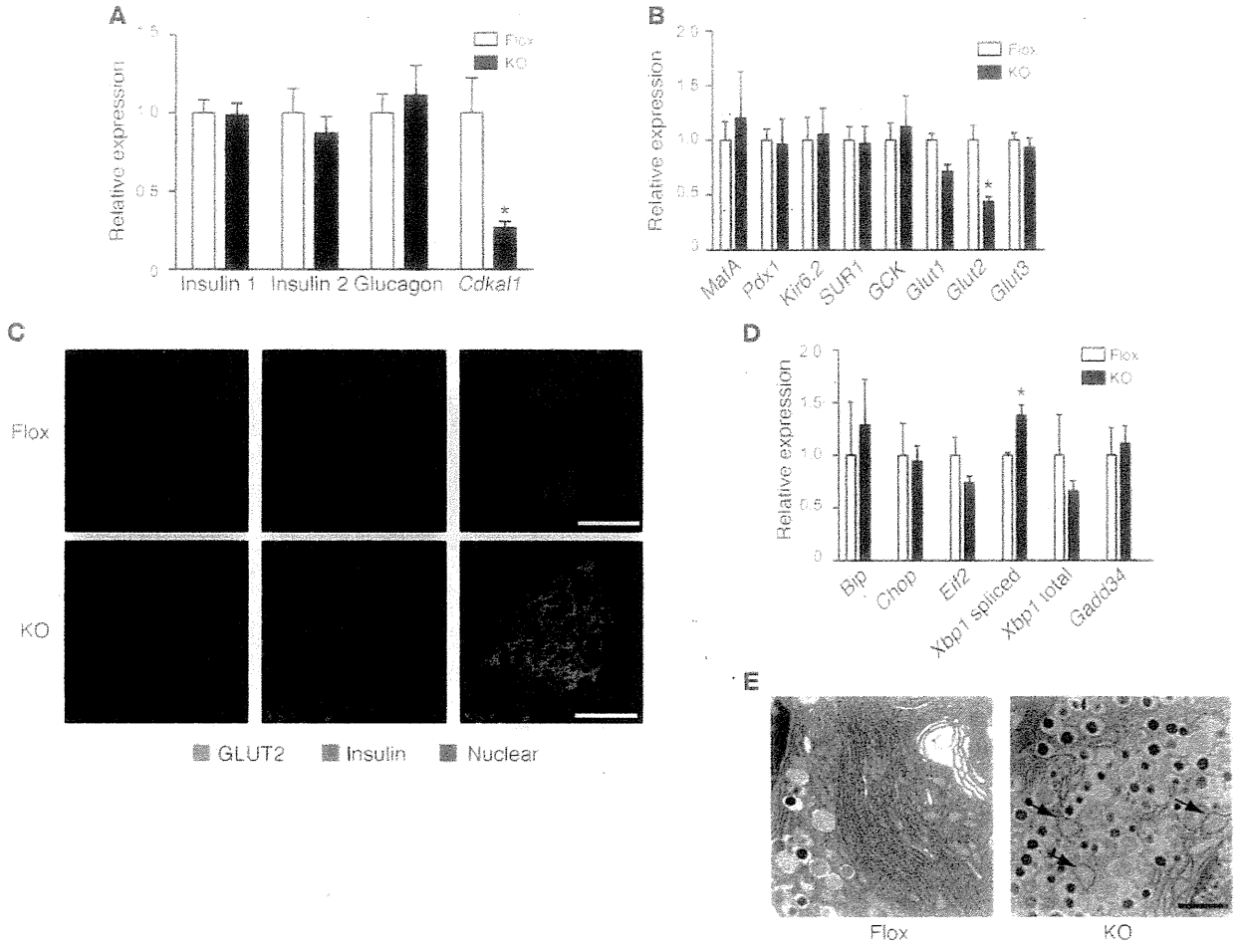

Figure 5

ER stress response in the pancreatic β cell KO mice. (**A**) Quantitative analysis of the mRNA expression of insulin, glucagon, and *Cdkal1* in isolated islets of β cell KO and Flox mice. $^*P < 0.05$; $n = 4$. (**B**) Comparison of the expression of β cell–related genes between β cell KO and Flox mice. $^*P < 0.05$; $n = 4$. (**C**) Subcellular distribution of GLUT2 in islets of β cell KO and Flox mice. Scale bars: 50 μm. (**D**) Quantitative analysis of ER stress–related genes in β cell KO and Flox mice. $^*P < 0.05$; $n = 4$. (**E**) Transmission electron microscopic examination of the ultrastructure of β cells in pancreatic sections of β cell KO mice and Flox mice. Arrows indicate the ER distention in the β cells of KO mice. Scale bar: 5 μm. Significant differences were examined by Student's *t* test (**A**, **B**, and **D**). All data are presented as mean ± SEM.

were fed either an HFD or a low-fat diet (LFD) for up to 8 weeks. There was no difference in weight gain between β cell KO and Flox mice during the experimental period (Figure 6A). Islet hypertrophy was observed in both β cell KO and Flox mice fed an HFD for 8 weeks as a compensatory effect of the diet (Supplemental Figure 12). However, significant glucose intolerance developed in β cell KO mice fed an HFD for 3 weeks, whereas Flox mice fed an HFD showed normal glucose tolerance compared with Flox mice fed an LFD (Figure 6B). Blood glucose levels at 15, 30, and 60 minutes after the intraperitoneal injection were higher in β cell KO mice than in Flox mice. After 8 weeks on an HFD, glucose intolerance was more severe in the β cell KO mice (Figure 6C). Blood glucose concentrations in β cell KO mice were continuously higher than control levels and increased 2 hours after a glucose injection (Figure 6C). In addition, both nonfasting blood glucose levels (Figure 6D) and 7 hour–fasting blood glucose levels (Figure 6E) were significantly higher in β cell KO mice than Flox mice after 3 weeks on an HFD, whereas nonfasting and 7 hour–fasting blood glucose levels in LFD-fed β cell KO mice were compatible with those in LFD-fed Flox mice (Figure 6, D and E). To investigate whether insulin sensitivity was affected in β cell KO mice, an insulin tolerance test was performed in β cell KO and Flox mice fed an HFD or LFD for 7 weeks. There were no differences in the action of insulin between β cell KO and Flox mice fed either diet (Figure 6F). We also investigated whether an HFD had any effect on liver function as well as counter-insulin responses such as glucagon production. To examine gluconeogenesis in the liver, Flox and β cell KO mice fed an HFD for 10 weeks were injected with pyruvate and blood glucose levels were measured. There was no significant difference in gluconeogenesis between Flox and β cell KO mice (Supplemental Figure 13A). Furthermore, we examined plasma glucagon levels in mice fed an HFD for 10 weeks. There was no difference in fasting glucagon levels between Flox and β cell KO mice (Supplemental Figure 13B). From these observations, we speculated that the severe glucose intolerance was mainly caused by HFD-induced ER stress and the consequent decrease in insulin secretion in Cdkal1

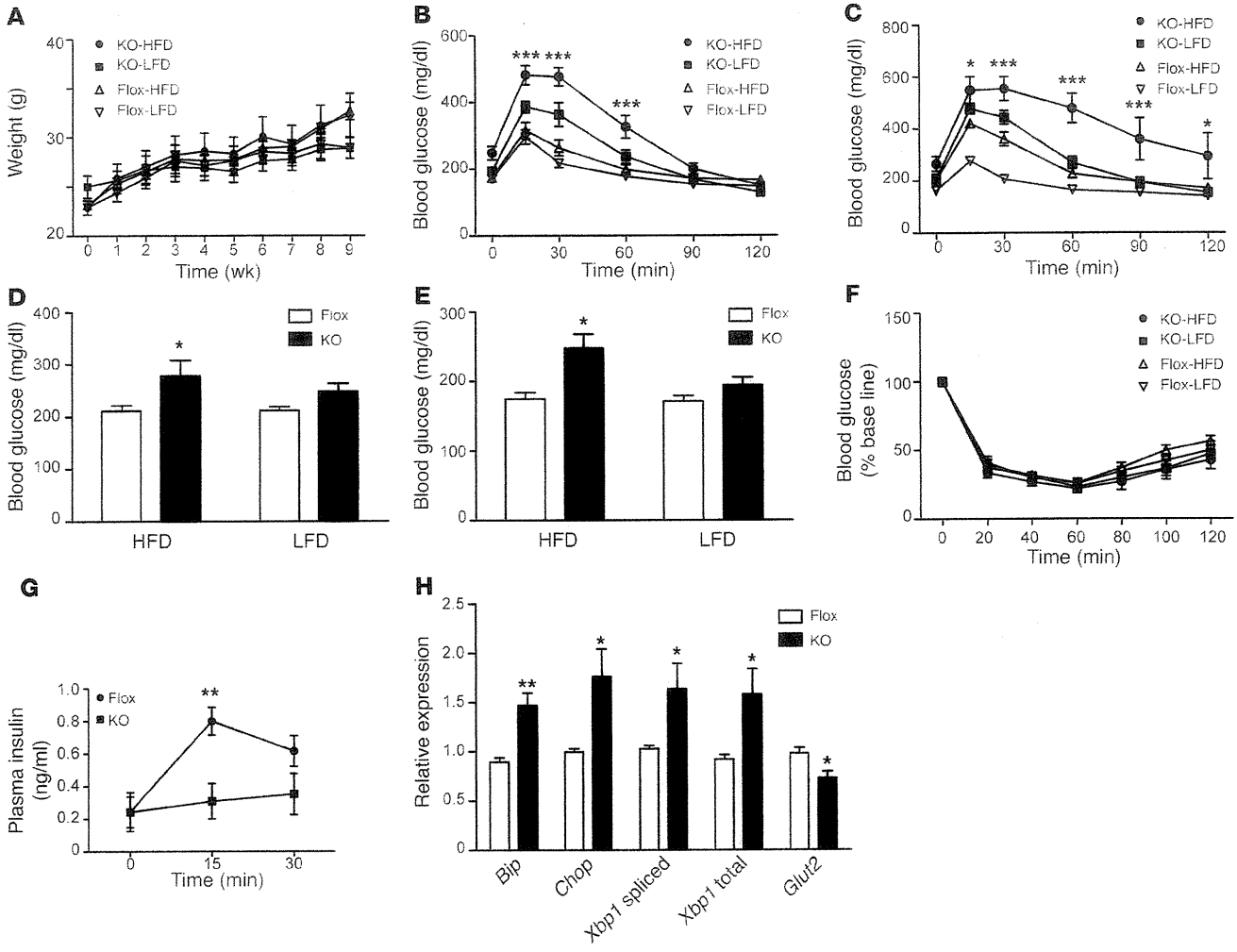

Figure 6

β cell KO mice exhibit increased ER stress and glucose intolerance after consuming an HFD. (**A**) Changes in body weight of β cell KO and Flox mice on an HFD and a LFD starting from 20 weeks old. (**B** and **C**) Results of the glucose tolerance test after 3 weeks (**B**) and 8 weeks (**C**) of consuming an HFD or a LFD. Mice were fasted for 7 hours from 8 am and injected with glucose (1 g/kg body weight). $^{*}P < 0.05$; $^{***}P < 0.001$, KO-HFD versus Flox-HFD mice. $n = 4$–6. (**D** and **E**) Nonfasting blood glucose (**D**) and 7-hour fasting blood glucose (**E**) levels after 3 weeks on an HFD or an LFD. $^{*}P < 0.05$; $n = 6$. (**F**) The insulin tolerance test was performed in mice fed an HFD or an LFD for 7 weeks. (**G**) β cell KO mice and Flox mice were fed an HFD for 8 weeks. Plasma insulin level during IPGTT (1 g/kg body weight) was examined in β cell KO mice and Flox mice fasted for 14 hours. $^{**}P < 0.01$; $n = 6$. (**H**) Relative expression of ER stress–related genes in β cell KO mice and Flox mice fed an HFD for 8 weeks. $^{**}P < 0.01$; $n = 4$–5. Significant differences between groups were examined by repeated measure of ANOVA (**A**–**C**, **F**, and **G**), 2-way ANOVA (**D** and **E**), or Student's *t* test (**H**). All data are presented as mean ± SEM.

KO β cells. Serum insulin levels after the injection of glucose were measured in β cell KO and Flox mice fed an HFD. Blood insulin levels after the challenge were significantly lower in β cell KO mice than in Flox mice (Figure 6G). Impaired glucose-stimulated insulin secretion was also observed in isolated Cdkal1-deficient pancreatic islets (Supplemental Figure 14). Finally, pancreatic islets were isolated from β cell KO mice and Flox mice fed the HFD for 8 weeks, and the expression levels of ER stress–related genes were examined (Figure 6H). We observed a significant increase in the expression of major ER stress–related genes, including the *Bip*, *CHOP*, and *Xbp1* genes. Our results indicate that Cdkal1 deficiency induces a massive ER stress response, which in turn decreases insulin secretion, causing severe glucose intolerance.

Discussion

Chemical modifications of nucleotides surrounding anticodons in tRNAs are believed to be essential for accuracy and efficiency in protein translation (14). The structural basis of the $ms^2i^6A^{37}$ modification at A^{37} of tRNA was recently identified in bacteria (30). The methylthiolation of i^6A^{37} is capable of stabilizing the codon-anticodon interaction through cross-strand stacking with the base of the first nucleotide of the mRNA codon. This stabilization of the codon-anticodon interaction prevents frame shifting and misreading during translation. In the present study, we showed that the ms^2t^6A modification of $tRNA^{Lys}$(UUU) by Cdkal1 is required for the accurate translation of AAA and AAG codons. The human insulin gene contains 2 Lys(AAG) codons. One of the Lys residues

is located at the cleavage site between the C-peptide and A chain of insulin. Misreading of this Lys codon during insulin synthesis by ms^2t^6A modification–deficient $tRNA^{Lys}(UUU)$ may cause the misfolding or miscleavage of proinsulin, which has an impact on glucose homeostasis. Indeed, we observed a decreased incorporation of lysine residue in Cdkal1-deficient β cells, as well as decreased C-peptide levels in pancreas of Cdkal1 KO. Interestingly, SNPs in the *Cdkal1* gene have been shown to associate with impaired conversion of proinsulin to insulin (31–33), supporting our finding that Cdkal1 deficiency may cause aberrant proinsulin generation.

The main role of pancreatic β cells is the adequate synthesis and release of insulin in response to glucose. To accomplish this task, the cells induce insulin biosynthesis in response to glucose. Proinsulin mRNA represents 20% of the total mRNA expression in glucose-stimulated β cells, whereas (pro)insulin biosynthesis approaches 50% of their total protein production (34, 35). It is inevitable that some insulin will be misfolded in such a mass production (36, 37). However, if augmented absolute levels of misfolded proinsulin are above the threshold, the misfolded proinsulin may lead to the inhibition of insulin production, ER stress, and β cell dysfunction. The onset of diabetes caused by misfolded proinsulin has been well studied in mutant INS gene–induced diabetes of youth (MIDY). In *Akita* mice, in which a heterozygous proinsulin-C(A7)Y mutation in the mouse *Ins2* gene is identical to the heterozygous mutation causing human MIDY, the mutant proinsulin in *Akita* mice blocks insulin production and activates ER stress in β cells (38, 39). On the other hand, dysregulation of protein synthesis can also lead to the production of misfolded proinsulin and ER stress. For example, a massive increase of protein synthesis by *Perk* deficiency causes massive proinsulin production, which leads to abnormal folding of proinsulin and ER stress (37). Taken together, these findings suggest that the absolute amount of misfolded proinsulin is a critical determinant of onset of ER stress followed by dysfunction of β cells. In β cell KO mice, the Cdkal1 deficiency may cause a certain amount of proinsulin to be mistranslated, which may be misfolded and accumulate in the ER, leading to further inhibition of insulin production and subsequent activation of ER stress.

A recent study showed impaired mitochondrial ATP generation, first-phase insulin exocytosis, and responsiveness of ATP-sensitive K^+ channel to glucose in general *Cdkal1*$^{-/-}$ mice (40). In β cell KO mice, we also observed impaired first-phase insulin secretion as well as impaired ATP generation after glucose stimulation (Figure 3H and Supplemental Figure 15). Considering the molecular function of Cdkal1, it is not assumed that Cdkal1 directly regulates these functions. These results suggest that aberrant protein translation may occur in the proteins involved in the regulation of mitochondrial ATP generation and insulin exocytosis in addition to insulin in Cdkal1-deficient mice. Although we did not detect obvious changes in the levels of Kir6.2 and SUR1, other proteins involved in mitochondrial functions may be abnormally translated and in turn cause the defect of ATP generation observed in KO islets.

In conclusion, our results suggest that functional loss of Cdkal1 affects the accuracy of protein translation, causing the synthesis of abnormal insulin, which triggers ER stress in β cells. These results provide evidence linking the molecular function of Cdkal1 with T2D.

Methods

Animals. Cdkal1$^{flox/flox}$ (Flox) mice were generated by flanking exon 5 of the *Cdkal1* gene with the loxP sequence (Supplemental Figure 8A). Flox mice were crossed with transgenic mice expressing Cre recombinase under the control of the rat insulin 2 promoter (RIP-Cre) to obtain pancreatic-specific Cdkal1 KO mice (Cdkal1$^{flox/flox;\ RIP\text{-}Cre/0}$; β cell KO). To delete Cdkal1 from all tissues, Flox mice were crossed with transgenic mice carrying Cre recombinase under the control of a CAG promoter (CAG-Cre) provided by RIKEN through a national bioresource project of the Ministry of Education, Culture, Sports, Science and Technology of Japan (MEXT). All mouse strains (Cdkal1$^{flox/flox}$, RIP-Cre, CAG-Cre) were backcrossed onto the C57BL/6 genetic background for more than 7 generations.

Animals were housed at 25°C with 12-hour light/12-hour dark cycles. High-fat chow (D12451, 45% kcal% fat) and low-fat chow (D12450B, 10% kcal% fat) were purchased from Research Diets. All animal procedures were approved by the Animal Ethics Committee of Kumamoto University (approval ID; A21-103).

Measurement of blood glucose and insulin levels. Mice were fasted for 14 hours (8:00 pm to 10:00 am) or 7 hours (8:00 am to 3:00 pm), followed by intraperitoneal injection of glucose (1 g/kg). Blood glucose was determined by a glucometer (ACCU-CHEK, Aviva; Roche). Plasma insulin or C-peptide levels were determined using an ELISA kit. To measure pancreatic C-peptide levels, whole pancreases were homogenized in an acid-ethanol solution. Pancreatic C-peptide levels were normalized to total protein concentration measured by BCA reagent (Pierce). For the insulin tolerance test, mice were injected with 1 unit/kg of regular human insulin. For pyruvate tolerance test, mice were fasted overnight and injected with sodium pyruvate (2 g/kg).

Morphological examination. For immunohistochemical examination, pancreatic sections were stained using anti-insulin (Santa Cruz Biotechnology Inc.), anti-glucagon (Sigma-Aldrich), and anti-GLUT2 (Santa Cruz Biotechnology Inc.) antibodies. Images were obtained using a FV1000 confocal microscope (Olympus). For islet morphological examination, pancreatic sections were examined as described previously (19). Pancreatic sections for transmission electron microscopic examination were prepared as described previously (41).

Gene expression studies. Islets were isolated from β cell KO mice or Flox mice by intraductal collagenase (Liberase TL grade; Roche) digestion followed by hand picking. Isolation of total RNA from islets was performed using an RNeasy Mini Kit (QIAGEN). A PrimerScript RT Reagent Kit was used to generate cDNA. Quantitative real-time PCRs were performed using either a TaqMan Gene Expression Kit (Applied Biosystems) or SYBR Premix Ex Taq. The results were normalized to the level of GAPDH or β actin. Primer sequences are provided in Supplemental Table 1.

Metabolic labeling experiments. Fifty islets were washed in Krebs-Ringer bicarbonate buffer (115 mM NaCl, 5 mM KCl, 10 mM $NaHCO_3$, 2.5 mM $MgCl_2$, 2.5 mM $CaCl_2$, and 20 mM HEPES, pH 7.4, 0.1% BSA) containing 2.8 mM glucose and incubated in the same buffer for 1 hour at 37°C. The buffer was then changed to incubation buffer (2.8 mM or 16.7 mM glucose) containing 100 μCi [^{35}S]-methionine and cysteine (Tran^{35}S-LABEL; MP Biomedical Inc.) for 1 hour. The islets were lysed in 100 μl of lysis buffer (50 mM HEPES, pH 7.4, 150 mM NaCl, 1% Triton X-100, 0.1% SDS, protease inhibitor cocktail; Roche). Then 5 μl of lysate was taken for a total protein assay using BCA reagent (Pierce), and 5 μl was taken for measurement of total protein synthesis by trichloroacetic acid precipitation on Whatman filter paper. Proinsulin synthesis was measured by immunoprecipitation of 50 μg of islet lysates with anti-insulin antibody (Santa Cruz Biotechnology Inc.) conjugated on protein A–Dynabeads (Invitrogen). Immunoprecipitated proteins were resolved on a Tris-Tricine gel (Invitrogen). The labeled proinsulin was quantified by FLP2000 (Fuji Film).

L-[^{14}C(U)]-lysine and L-[3,4,5-^{3}H(N)-leucine were purchased from PerkinElmer Life and Analytical Sciences. Fifty islets were washed in Krebs-Ringer bicarbonate buffer containing 2.8 mM glucose. The buffer was changed to incubation buffer (16.7 mM glucose) containing 10 μCi of L-[3,4,5-^{3}H(N)-leucine and 1 μCi L-[^{14}C(U)]-lysine for 1 hour. The islets were lysed

in 50 μl of lysis buffer (50 mM HEPES, pH 7.4, 150 mM NaCl, 0.5% Triton X-100, protease inhibitor cocktail; Roche). Lysates were precleared with Dynabeads Protein A for 1 hour to reduce background absorption to Dynabeads. Lysates were then incubated with guinea pig anti-insulin antibody (AB3440; Millipore) for 3 hours, and (pro)insulin was immunoprecipitated by adding Dynabeads Protein A. Immunoprecipitated proteins was eluted using nondenaturing elution buffer included in the Dynabeads immunoprecipitation kit (Invitrogen), and radioactivity was measured by a liquid scintillation counter (Aloka).

Analysis of ms^2t^6A modification in tRNA. Purification of total RNA from mouse tissues or a cultured cell line was performed using a guanidinium thiocyanate/phenol/chloroform method (42). Individual $tRNA^{Lys}$(UUU) or $tRNA^{Lys}$(CUU) was purified by reciprocal circulating chromatography (RCC) (43). Purified total RNA or individual tRNA was hydrolyzed to obtain nucleosides or digested to obtain oligonucleotides, then subjected to liquid chromatography/mass spectrometry (44).

Reporter assay for detecting frame-shifts in B. subtilis. Reporters for detecting translational fidelity were adapted from a luciferase-based reporter as described previously (16). For protein expression in *B. subtilis*, reporters were cloned into pHT01 vectors (MoBiTec). WT (trpC2) *B. subtilis* and *yqeV*-deficient (Δ*yqeV*) *B. subtilis* were obtained from the National BioResource Project (*B. subtilis*; NIG). Transformation of *B. subtilis* with a pHT01 vector containing each construct was performed according to the protocol of Anagnostopoulos and Spizizen (45). Colonies were cultured at 37°C in 2 ml LB medium containing 2.5 μg/ml chloramphenicol until OD_{600} = 0.5. Isopropyl β-D-1thiogalactopyranoside (IPTG) was added to cultures at a final concentration of 1 mM. After 1 hour of incubation, the cultures were harvested and lysed in lysis buffer (50 mM HEPES, pH 7.4, 100 mM KCl, 10 mM $MgCl_2$, 2 mg/ml lysozyme). Aliquots of 5 μl were used in the luciferase assay using the Dual-Luciferase Reporter Assay System (Promega).

Islet perifusion. Islets were isolated from Flox mice or β cell KO mice and cultured in RPMI medium with 10% FBS overnight. Seventy islets were loaded on a filter (Millipore) and perifused with KRB buffer with constant bubbling of 95% O_2 and 5% CO_2 for 30 minutes. Islets were then stimulated with KRB buffer containing 16.7 mM glucose. Islets were perifused with KRB buffer at a flow rate of 1 ml/min. Insulin levels were measured by ELISA as described above.

Biochemical assay. Western blotting was carried out as described elsewhere. The anti-Kir6.2 antibody was purchased from Sigma-Aldrich, anti-SUR1 antibody was from Santa Cruz Biotechnology Inc., and anti-Pdx1 antibody was from Millipore. ATP levels were measured in 25 islets using an ATP Bioluminescent Kit (Roche). Briefly, islets were incubated in KRB buffer containing 2.8 mM glucose for 30 minutes and then stimulated with KRB buffer containing either 2.8 mM glucose or 16.7 mM glucose for 30 minutes. The extraction and measurement of ATP in islets were performed according to protocols provided.

Statistics. All data are presented as mean ± SEM. Statistical significance of differences between groups was evaluated using 1-way ANOVA, 2-way ANOVA, repeated measure of 2-way ANOVA, 2-tailed Student's *t* test, and the Mann-Whitney *U* test. $P < 0.05$ was considered significant.

Acknowledgments

We thank E. Araki and T. Kondo for help with the immunohistochemistry, K. Asai for providing the materials and the technical advice for transformation of *B. subtilis*, and N. Maeda for technical assistance. This work was supported by a Grant-in-Aid for Scientific Research from the Ministry of Education, Culture, Sports, Science and Technology of Japan, by the Japan Society for the Promotion of Science (JSPS) through its Funding Program for Next Generation World-Leading Researchers, by the Uehara Memorial Foundation, and by the Takeda Science Foundation.

Received for publication March 17, 2011, and accepted in revised form June 8, 2011.

Address correspondence to: Kazuhito Tomizawa, Department of Molecular Physiology, Faculty of Life Sciences, Kumamoto University, 1-1-1 Honjyo, Kumamoto 860-8556, Japan. Phone: 81.96.373.5050; Fax: 81.96.373.5052; E-mail: tomikt@kumamoto-u.ac.jp.

1. Steinthorsdottir V, et al. Variant in CDKAL1 influences insulin response and risk of type 2 diabetes. *Nat Genet.* 2007;39(6):770–775.
2. Saxena R, et al. Genome-wide association analysis identifies loci for type 2 diabetes and triglyceride levels. *Science.* 2007;316(5829):1331–1336.
3. Scott LJ, et al. A genome-wide association study of type 2 diabetes in Finns detects multiple susceptibility variants. *Science.* 2007;316(5829):1341–1345.
4. Zeggini E, et al. Replication of genome-wide association signals in UK samples reveals risk loci for type 2 diabetes. *Science.* 2007;316(5829):1336–1341.
5. Dehwah MA, Wang M, Huang QY. CDKAL1 and type 2 diabetes: a globalmeta-analysis. *Genet Mol Res.* 2010;9(2):1109–1120.
6. Groenewoud MJ, et al. Variants of CDKAL1 and IGF2BP2 affect first-phase insulin secretion during hyperglycaemic clamps. *Diabetologia.* 2008;51(9):1659–1663.
7. Stancáková A, et al. Association of 18 confirmed susceptibility loci for type 2 diabetes with indices of insulin release, proinsulin conversion, and insulin sensitivity in 5,327 nondiabetic Finnish men. *Diabetes.* 2009;58(9):2129–2136.
8. Ruchat SM, et al. Association between insulin secretion, insulin sensitivity and type 2 diabetes susceptibility variants identified in genome-wide association studies. *Acta Diabetol.* 2009;46(3):217–226.
9. Arragain S, et al. Identification of eukaryotic and prokaryotic methylthiotransferase for biosynthesis of 2-methylthio-N6-threonylcarbamoyladenosine in tRNA. *J Biol Chem.* 2010; 285(37):28425–28433.
10. Pierrel F, Douki T, Fontecave M, Atta M. MiaB protein is a bifunctional radical-S-adenosylmethionine enzyme involved in thiolation and methylation of tRNA. *J Biol Chem.* 2004;279(46):47555–47563.
11. Hernandez HL, et al. MiaB, a bifunctional radical-S-adenosylmethionine enzyme involved in the thiolation and methylation of tRNA, contains two essential [4Fe-4S] clusters. *Biochemistry.* 2007; 46(17):5140–5147.
12. Urbonavicius J, Qian Q, Durand JM, Hagervall TG, Björk GR. Improvement of reading frame maintenance is a common function for several tRNA modifications. *EMBO J.* 2001;20(17):4863–4873.
13. Wilson RK, Roe BA. Presence of the hypermodified nucleotide N6-(delta2-isopentenyl)-2-methylthioadenosine prevents codon misreading by Escherichiacoli phenylalanyl-transfer RNA. *Proc Natl Acad Sci U S A.* 1989;86(2):409–413.
14. Agris PF. Decoding the genome: a modified view. *Nucleic Acids Res.* 2004;32(1):223–238.
15. Grosjean H, Sprinzl M, Steinberg S. Posttranscriptionally modified nucleosides in transfer RNA: their locations and frequencies. *Biochimie.* 1995;77(1-2):139–141.
16. Kimura S, Suzuki T. Fine-tuning of the ribosomal decoding center by conserved methyl-modifications in the Escherichia coli 16S rRNA. *Nucleic Acids Res.* 2010;38(4):1341–1352.
17. Kramer EB, Vallabhaneni H, Mayer LM, Farabaugh PJ. A comprehensive analysis of translational missense errors in the yeast Saccharomyces cerevisiae. *RNA.* 2010;16(9):1797–1808.
18. Kramer EB, Farabaugh PJ. The frequency of translational misreading errors in E. coli is largely determined by tRNA competition. *RNA.* 2007; 13(1):87–96.
19. Wei FY, et al. Cdk5-dependent regulation of glucose-stimulated insulin secretion. *Nat Med.* 2005; 11(10):1104–118.
20. Ching YP, Pang AS, Lam WH, Qi RZ, Wang JH. Identification of a neuronal Cdk5 activator-binding protein as Cdk5 inhibitor. *J Biol Chem.* 2002; 277(18):15237–15240.
21. Wang X, Ching YP, Lam WH, Qi Z, Zhang M, Wang JH. Identification of a common protein association region in the neuronal Cdk5 activator. *J Biol Chem.* 2000;275(41):31763–31769.
22. Back SH, et al. Translation attenuation through eIF2alpha phosphorylation prevents oxidative stress and maintains the differentiated state in beta cells. *Cell Metab.* 2009;10(1):13–26.
23. Eizirik DL, Cnop M. ER stress in pancreatic beta cells: the thin red line between adaptation and failure. *Sci Signal.* 2010;3(110):pe7.
24. Oslowski CM, Urano F. The binary switch between life and death of endoplasmic reticulum-stressed beta cells. *Curr Opin Endocrinol Diabetes Obes.* 2010; 17(2):107–112.
25. Scheuner D, Kaufman RJ. The unfolded protein response: a pathway that links insulin demand

with beta-cell failure and diabetes. *Endocr Rev.* 2008; 29(3):317–333.
26. Han D, et al. IRE1alpha kinase activation modes control alternate endoribonuclease outputs to determine divergent cell fates. *Cell.* 2009; 138(3):562–575.
27. Scheuner D, et al. Control of mRNA translation preserves endoplasmic reticulum function in beta cells and maintains glucose homeostasis. *Nat Med.* 2005;11(7):757–764.
28. Sachdeva MM, et al. Pdx1 (MODY4) regulates pancreatic beta cell susceptibility to ER stress. *Proc Natl Acad Sci U S A.* 2009;106(45):19090–19095.
29. Miyaki K, et al. Association of a cyclin-dependent kinase 5 regulatory subunit-associated protein 1-like 1 (CDKAL1) polymorphism with elevated hemoglobin A_1(c) levels and the prevalence of metabolic syndrome in Japanese men: interaction with dietary energy intake. *Am J Epidemiol.* 2010; 172(9):985–991.
30. Jenner LB, Demeshkina N, Yusupova G, Yusupov M. Structural aspects of messenger RNA reading frame maintenance by the ribosome. *Nat Struct Mol Biol.* 2010;17(5):555–560.
31. Kirchhoff K, et al. Polymorphisms in the TCF7L2, CDKAL1 and SLC30A8 genes are associated with impaired proinsulin conversion. *Diabetologia.* 2008; 51(4):597–601.
32. Stancáková A, et al. Association of 18 confirmed susceptibility loci for type 2 diabetes with indices of insulin release, proinsulin conversion, and insulin sensitivity in 5,327 nondiabetic Finnish men. *Diabetes.* 2009;58(9):2129–213.
33. Haupt A, et al. The risk allele load accelerates the age-dependent decline in beta cell function. *Diabetologia.* 2009;52(3):457–462.
34. Van Lommel L, et al. Probe-independent and direct quantification of insulin mRNA and growth hormone mRNA in enriched cell preparations. *Diabetes.* 2006;55(12):3214–3220.
35. Schuit FC, In't Veld PA, Pipeleers DG. Glucose stimulates proinsulin biosynthesis by a dose-dependent recruitment of pancreatic beta cells. *Proc Natl Acad Sci U S A.* 1988;85(11):3865–3869.
36. Schubert U, Antón LC, Gibbs J, Norbury CC, Yewdell JW, Bennink JR. Rapid degradation of a large fraction of newly synthesized proteins by proteasomes. *Nature.* 2000;404(6779):770–774.
37. Liu M, Li Y, Cavener D, Arvan P. Proinsulin disulfide maturation and misfolding in the endoplasmic reticulum. *J Biol Chem.* 2005;280(14):13209–13212.
38. Wang J, et al. A mutation in the insulin 2 gene induces diabetes with severe pancreatic beta-cell dysfunction in the Mody mouse. *J Clin Invest.* 1999; 103(1):27–37.
39. Yoshioka M, Kayo T, Ikeda T, Koizumi A. A novel locus, Mody4, distal to D7Mit189 on chromosome 7 determines early-onset NIDDM in nonobese C57BL/6 (Akita) mutant mice. *Diabetes.* 1997; 46(5):887–894.
40. Ohara-Imaizumi M, et al. Deletion of CDKAL1 affects mitochondrial ATP generation and first-phase insulin exocytosis. *PLoS One.* 2010; 5(12):e15553.
41. Han XJ, et al. CaM kinase I alpha-induced phosphorylation of Drp1 regulates mitochondrial morphology. *J Cell Biol.* 2008;182(3):573–585.
42. Chomczynski P, Sacchi N. The single-step method of RNA isolation by acid guanidinium thiocyanate-phenol-chloroform extraction: twenty-something years on. *Nat Protoc.* 2006;1(2):581–585.
43. Miyauchi K, Ohara T, Suzuki T. Automated parallel isolation of multiple species of non-coding RNAs by the reciprocal circulating chromatography method. *Nucleic Acids Res.* 2007;35(4):e24.
44. Ikeuchi Y, et al. Agmatine-conjugated cytidine in a tRNA anticodon is essential for AUA decoding in archaea. *Nat Chem Biol.* 2010:6(4):277–282.
45. Anagnostopoulos C, Spizizen J. Requirement for Transformation in Bacillus subtilis. *J Bacteriol.* 1961:81(5):741–746.

Diabetol Int (2011) 2:208–213
DOI 10.1007/s13340-011-0046-7

ORIGINAL ARTICLE

Clinical features of Japanese type 2 diabetics with insulinogenic index in normal range after treatment of glucotoxicity

Hiromi Iwahashi · Etsuko Fukuda-Akita · Ayumi Fukuda-Tokunaga · Kohei Okita · Yukio Horikawa · Akihisa Imagawa · Tohru Funahashi · Iichiro Shimomura · Kazuya Yamagata

Received: 19 April 2011 / Accepted: 11 September 2011 / Published online: 20 October 2011

Abstract Early phase insulin secretion has been reported to be impaired in patients with type 2 diabetes and to remain subnormal even after treatment of the glucotoxicity. We evaluated insulin secretion profiles by performing a 75-g oral glucose tolerance test (OGTT) in 178 Japanese patients with type 2 diabetes after minimizing the influence of glucotoxicity with diet or insulin therapy during hospitalization. Among the 178 patients, 161 (90.4%) had a low insulinogenic index (I.I.; < 0.4) and 17 (9.6%) had an index in the normal range (I.I. ≥ 0.4). This normal I.I. group was characterized by visceral obesity and insulin resistance, and showed delayed insulin secretion. Their total insulin response was significantly increased compared with that of the low response group or the normal glucose tolerance (NGT) group. Strikingly, in the normal I.I. group, one patient improved to the stage of NGT and three to impaired glucose tolerance (IGT) after treatment of the glucotoxicity. These results indicate that some patients will show a normal insulinogenic index after treatment of the glucotoxicity.

Keywords Type 2 diabetes · Early insulin secretion · Insulinogenic index · Visceral obesity

H. Iwahashi · E. Fukuda-Akita · A. Fukuda-Tokunaga · K. Okita · A. Imagawa · T. Funahashi · I. Shimomura
Department of Metabolic Medicine, Graduate School of Medicine, Osaka University, Osaka, Japan

Y. Horikawa
Department of Diabetes and Endocrinology, Graduate School of Medicine, Gifu University, Gifu, Japan

K. Yamagata (✉)
Department of Medical Biochemistry, Faculty of Medical and Pharmaceutical Sciences, Kumamoto University, 1-1-1 Honjo, Kumamoto 860-8556, Japan
e-mail: k-yamaga@kumamoto-u.ac.jp

Introduction

Early phase insulin secretion in response to glucose is important for maintaining normal glucose tolerance, and this early response is characteristically impaired in patients with type 2 diabetes [1–3]. Genetic factors are important determinants of early phase insulin secretion, although a number of environmental and metabolic conditions also influence early phase secretion [1, 4, 5]. Chronic hyperglycemia is a well-known metabolic determinant. Chronic hyperglycemia exerts a detrimental effect on the insulin secretion capacity, including early phase; this phenomenon has been called glucotoxicity [1–3, 6]. An important characteristic of glucotoxicity is that it can be partly recovered by treatment of the hyperglycemia [7–10].

The insulinogenic index (I.I.) is calculated as the increment of plasma insulin compared with that of glucose at 30 min after the glucose load in the oral glucose tolerance test (OGTT), and it is widely used to estimate early phase insulin secretion. A low I.I. is generally defined as an index below 0.4 (75-g OGTT) or 0.5 (100-g OGTT), and diabetic patients have a low index value [11, 12]. Recently, we examined the insulin response to the 75-g OGTT in Japanese patients with type 2 diabetes after improvement of glucotoxicity and found that the I.I. was significantly lower in diabetic patients compared with subjects who had normal glucose tolerance (NGT) (0.17 ± 0.01 vs. 0.77 ± 0.04, $p < 0.0001$) [13]. Our analysis also revealed that 10.9% (21/192) of the diabetic patients had an I.I. in the normal range (I.I. ≥ 0.4) according to the 75-g OGTT. Although the impaired response of insulin is somewhat improved by treatment of hyperglycemia, the insulin response of patients with type 2 diabetes has been reporetd to remain subnormal even after the treatment of glucotoxicity [7, 8]. In the present study, we investigated the

clinical characteristics of Japanese diabetics who displayed normal I.I. values.

Research design and methods

Subjects

We enrolled 192 unrelated Japanese patients with type 2 diabetes who were admitted to Osaka University Hospital for improvement of glycemic control from 2001 to 2005 [13]. After hospitalization, the patients were treated by diet alone, or diet plus sulfonylurea, or insulin. Since the effects of sulfonylurea may remain in insulin secretion of beta cells, we excluded data of patients who were treated by sulfonylurea during hospitalization from the analysis. After this, we analyzed 178 patients, of whom 48 were treated with diet alone and 130 with diet and insulin after hospitalization to decrease glucotoxicity. The clinical characteristics of the analyzed patients are shown in Table 1. Diet therapy consists of daily calorie intake with 25–30 kcal/day per ideal body weight, the nutrient contents of which are about 60% carbohydrates, 25% lipids, and 15% protein. Treatment was continued for at least 2 weeks until the fasting plasma glucose (FPG) level was below 126 mg/dl (7.0 mmol/l) [13] for decreasing the influence of

Table 1 Clinical characteristics of the study subjects

	I.I. ≥ 0.4	I.I. < 0.4	NGT	*p* value		
				I.I. ≥ 0.4 vs. I.I. < 0.4	NGT vs. I.I. ≥ 0.4	NGT vs. I.I. < 0.4
At the time of hospitalization						
N (male/female)	17 (9/8)	161 (86/75)	275 (193/82)	NS	NS	0.0006
Age (years)	56.2 ± 3.3	59.0 ± 0.9	54.1 ± 0.5	NS	NS	<0.0001
Duration (years)	8.4 ± 1.9	11.4 ± 0.8		NS		
Family history (±)	7/10 (n = 17)	75/57 (n = 132)		NS		
BMI (kg/m^2)	29.4 ± 1.8	24.3 ± 0.3	22.8 ± 0.2	0.0002	<0.0001	<0.0001
Max BMI before onset (kg/m^2)	33.3 ± 2.0 (n = 15)	28.0 ± 0.4 (n = 154)		0.0004		
Waist circumference (cm)	100.5 ± 4.1	89.0 ± 1.0	81.5 ± 0.5	0.0016	<0.0001	<0.0001
VFA (cm^2)	141.5 ± 19.0 (n = 12)	97.7 ± 5.9 (n = 89)		0.0144		
HbA1c (%)	8.8 ± 0.4	9.1 ± 0.1	5.1 ± 0.1 (n = 44)	NS	<0.0001	<0.0001
FPG (mg/dl)	166.0 ± 11.5	171.9 ± 3.9	93.5 ± 0.4	NS	<0.0001	<0.0001
Fasting insulin (μU/ml)	16.6 ± 1.9	8.1 ± 0.5 (n = 143)	4.8 ± 0.2	<0.0001	<0.0001	<0.0001
HOMA-IR	6.62 ± 0.80	3.46 ± 0.21 (n = 143)	1.12 ± 0.05	<0.0001	<0.0001	<0.0001
SBP (mmHg)	130.5 ± 4.3	129.5 ± 1.2	119.8 ± 1.1	NS	0.0160	<0.0001
DBP (mmHg)	80.9 ± 3.9	73.3 ± 0.8	71.8 ± 0.8	0.0078	0.0051	NS
Triglycerides (mg/dl)	214.5 ± 23.3	154.9 ± 9.3	114.6 ± 4.7	0.0037	<0.0001	<0.0001
HDL-cholesterol (mg/dl)	42.5 ± 2.2	48.9 ± 1.1	54.7 ± 1.0	NS	0.0027	0.0001
FFA (μEq/l)	247.0 ± 34.3	299.6 ± 12.3		NS		
Adiponectin (μg/ml)	3.9 ± 0.7 (n = 13)	5.1 ± 0.3 (n = 124)		NS		
Urinary CPR (μg/day)	72.4 ± 10.5	63.0 ± 3.6		NS		
Antidiabetic medication (diet/OHA/insulin)	7/6/4	29/107/25		0.0297		
At the time of OGTT						
FPG (mg/dl)	116.0 ± 4.3	118.9 ± 1.7	93.5 ± 0.4	NS	<0.0001	<0.0001
Fasting IRI (μU/ml)	14.9 ± 1.7	7.1 ± 0.4	4.8 ± 0.2	<0.0001	<0.0001	<0.0001
Insulinogenic index	0.56 ± 0.05	0.12 ± 0.01	0.77 ± 0.04	<0.0001	NS	<0.0001
HOMA-IR	4.24 ± 0.49	2.08 ± 0.12	1.12 ± 0.05	<0.0001	<0.0001	<0.0001

Data are mean ± SE

NS not significant, *OHA* oral hypoglycemic agent

glucotoxicity. Informed consent was obtained from all participants for the various examinations. Before measurement of the plasma adiponectin level, written informed consent was obtained from each subject. Approval of the ethics committee of Osaka University was also obtained.

A total of 275 subjects with normal glucose tolerance (NGT) were selected among people undergoing annual health examinations at the institutions participating in the Japanese Visceral Fat Syndrome (J-VFS) Study [14]. Normal glucose tolerance was confirmed by the results of a 75-g OGTT. Written informed consent was also obtained from all of the NGT subjects.

Measurements

At the time when FPG was below 126 mg/dl after treatment of hyperglycemia, a 75-g OGTT was performed following an overnight fast. Treatment with insulin was postponed until the end of the OGTT. Blood samples were collected at 0, 30, 60, and 120 min. The insulinogenic index was calculated as the ratio of the increment of insulin to that of plasma glucose at 30 min after the glucose load (Δinsulin 0–30 min/ΔPG 0–30 min) and was used to assess early phase insulin secretion [1]. Homeostasis model assessment of insulin resistance (HOMA-IR) was employed to estimate insulin sensitivity and was calculated as follows: [fasting plasma glucose (mg/dl)] × [fasting IRI (μU/ml)]/405 [15]. The glucagon stimulation test was performed by infusing 1 mg of glucagon (Novo Nordisk Pharma. Ltd., Tokyo, Japan) intravenously after an overnight fast. Blood samples were collected at 0 and 5 min. Plasma glucose concentrations were measured by the glucose oxidase method, while immunoreactive insulin (IRI) and C-peptide levels were measured with enzyme immunoassay kits. Plasma adiponectin levels were determined with an adiponectin ELISA kit (Otsuka Pharmaceutical Co. Ltd., Tokushima, Japan) as described previously [16]. HbA1c was determined by high-performance liquid chromatography. The value of HbA1c (%) was estimated as the NGSP equivalent value (%) calculated by the formula HbA1c (%) = HbA1c (JDS)(%) + 0.4%, considering the relational expression of HbA1c (JDS) (%) measured by the previous Japanese standard substance and measurement methods and HbA1c (NGSP) [17].

Statistical analysis

Data are presented as the mean ± standard error (SE). Data on triglycerides, adiponectin, and the insulinogenic index were logarithmically transformed (log10) before statistical analysis because their distributions were skewed. Comparison of variables between groups was done with the two-tailed Student's t test or the Mann-Whitney nonparametric test, while comparison of frequencies was performed by the chi-square test. For all analyses, Statview 5.5 software was employed, and $p < 0.05$ was considered to indicate significance.

Results

Table 1 shows the clinical characteristics of the high and low response groups at the time of hospitalization and the OGTT. It was found that 161 (90.4%) of the 178 diabetic patients had a low insulinogenic index (I.I. < 0.4), while the I.I. was within the normal range (≥ 0.4) in 17 (9.6%) patients. These 17 patients were being treated by diet ($n = 7$) or insulin ($n = 10$), and insulin was discontinued on the morning of the OGTT. The average I.I. of the low response group (I.I. < 0.4) and the high response group (I.I. ≥ 0.4) was 0.12 ± 0.01 and 0.56 ± 0.05, respectively ($p < 0.0001$). The I.I. of the high response group was similar to that of the control group (0.77 ± 0.04). The distribution of age, sex, and the duration of type 2 diabetes was similar between the two groups. A family history of type 2 diabetes (at least one diabetic among second-degree relatives) tends to be less common in the high response group, but not significantly (41.2 vs. 56.8%, $p = 0.2224$). Strikingly, body mass index (BMI) was significantly greater in the high response group compared with the low response group (29.4 ± 1.8 vs. 24.3 ± 0.3, $p = 0.0002$). Furthermore, the maximal BMI (33.3 ± 2.0 vs. 28.0 ± 0.4, $p = 0.0004$), waist circumference (100.5 ± 4.1 vs. 89.0 ± 1.0, $p = 0.0013$), and visceral fat area (VFA) (141.5 ± 19.0 vs. 97.7 ± 5.9, $p = 0.0144$) were also significantly greater in the high response group, indicating that the high response group had visceral fat obesity. Generally, visceral fat obesity is associated with insulin resistance. In agreement with this, both the fasting insulin level (16.6 ± 1.9 vs. 8.1 ± 0.5, $p < 0.0001$) and HOMA-IR (6.62 ± 0.80 vs. 3.46 ± 0.21, $p < 0.0001$) at the time of hospitalization were significantly higher in the high response group compared with the low response group, while the plasma adiponectin level was not significantly different between the two groups. These data indicate that the high response group had the characteristic features of insulin resistance. FPG and HbA1c levels did not differ between the two groups.

Figure 1 shows the plasma glucose and insulin profiles obtained during the 75-g OGTT for the high response group ($n = 17$), the low response group ($n = 161$), and the NGT group ($n = 275$). Both the high and low response groups showed a diabetic pattern. FPG was significantly higher in the high response group (116.0 ± 4.3 mg/dl, $p < 0.0001$) and the low response group (119.0 ± 1.6 mg/dl, $p < 0.0001$) than in the control (NGT) group (93.5 ± 0.4 mg/dl), and the glucose levels at 30, 60, and

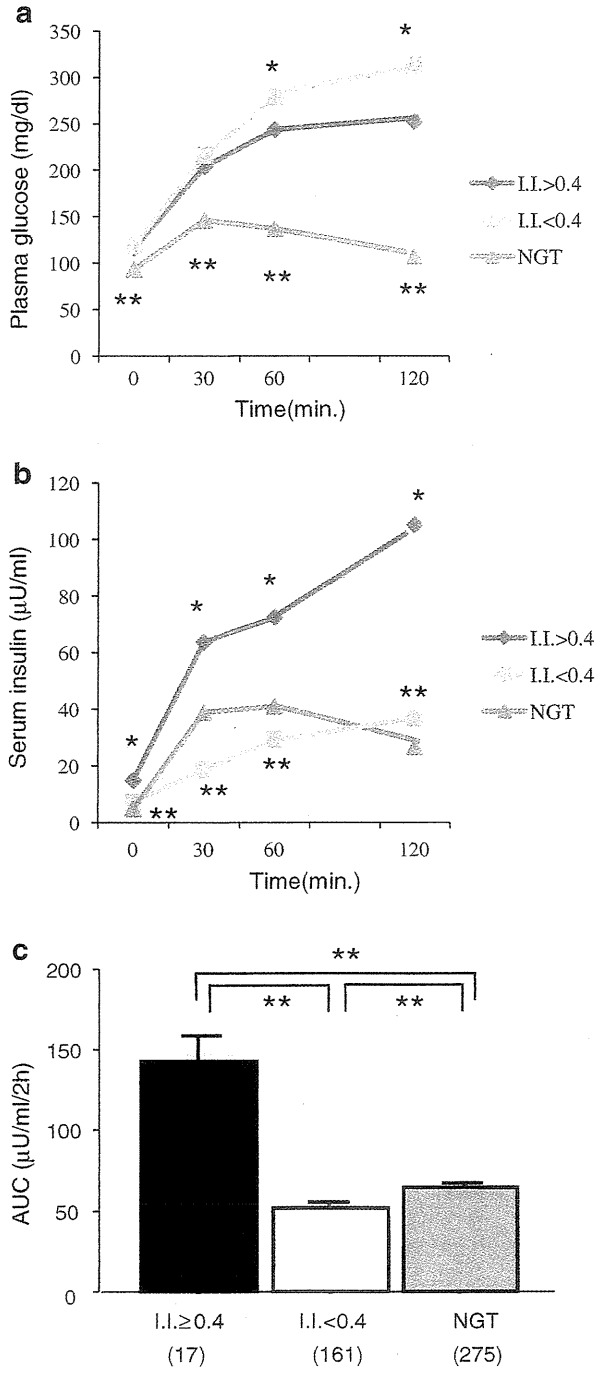

Fig. 1 Plasma glucose (**a**) and serum insulin (**b**) profiles during the 75-g OGTT in the NGT group (*filled triangles*), the high response diabetic group (I.I. ≥ 0.4; *filled diamonds*), and the low response diabetic group (I.I. < 0.4; *filled squares*). **a** $*p < 0.005$ versus the low response diabetic group. $**p < 0.0001$ versus the both diabetic groups. **b** $*p < 0.0005$ versus NGT and the low response diabetic group. $**p < 0.0001$ versus NGT group. **c** AUC ($insulin_{0-120}$) of the diabetic groups and the NGT group. Data are the mean ± SEM. $**p < 0.001$

120 min were also significantly higher in the diabetics (Fig. 1a). Although there were no significant differences of FPG and the glucose level at 30 min between the high response group and the low response group, the glucose levels at 60 min (243.8 ± 8.7 vs. 279.0 ± 3.9, $p = 0.0049$) and 120 min (252.2 ± 16.7 vs. 313.2 ± 5.6, $p < 0.0010$) were significantly lower in the high response group (Fig. 1a). Serum insulin levels measured during the OGTT are shown in Fig. 1b. At 0 and 120 min, insulin levels were significantly increased in the low response group compared with the control (NGT) group, whereas the insulin levels at 30 and 60 min were significantly lower in the diabetic group, indicating the blunted and delayed insulin response that is characteristics of type 2 diabetes. Interestingly, the insulin secretion pattern of the high response group was different, and the serum insulin level of this group was significantly higher at all times compared with that of the NGT group. Insulin levels at 30 min (high response group 63.7 ± 6.4; NGT group 38.9 ± 1.6, $p = 0.0002$), 60 min (high response group 72.5 ± 11.4; NGT group 41.0 ± 1.8, $p < 0.0001$), 0 min (high response group 14.9 ± 1.7; NGT group 4.8 ± 0.2, $p < 0.0001$), and 120 min (high response group 105.1 ± 15.3; NGT group 26.7 ± 1.0, $p < 0.0001$) were significantly higher in the high response group. Figure 1c shows the area under the concentration versus time curve (AUC) of serum insulin during the OGTT [AUC ($insulin_{0-120}$)]. The AUC ($insulin_{0-120}$) of the high response group was significantly increased compared with that of the NGT group ($p < 0.0001$) and that of the low response group ($p < 0.0001$). Figure 2 shows the ΔCPR levels in the glucagon test. Insulin secretion (estimated by ΔCPR) was also significantly increased in the high response group

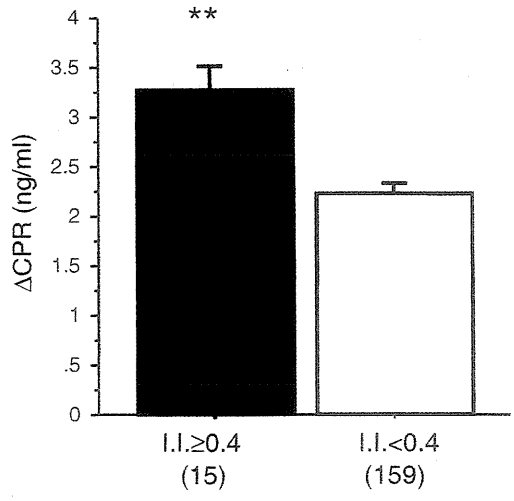

Fig. 2 ΔCPR of the diabetic subjects during the glucagon test. Data are the mean ± SEM. $**p < 0.005$